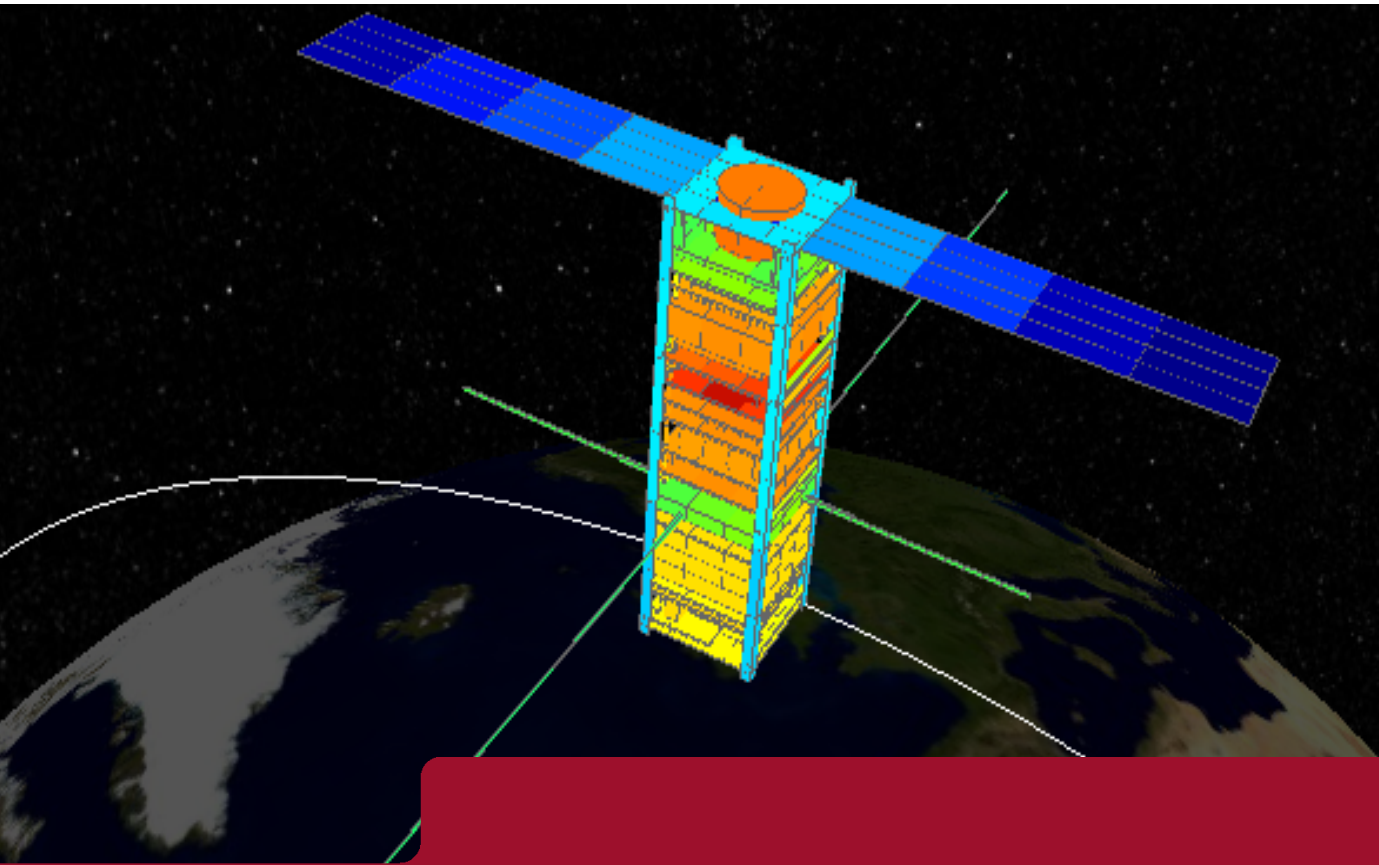




DEGREE PROJECT IN SPACE TECHNOLOGY,
SECOND CYCLE, 30 CREDITS
STOCKHOLM, SWEDEN 2016

Thermal Analysis and Control of MIST CubeSat

SHREYAS CHANDRASHEKAR



KTH ROYAL INSTITUTE OF TECHNOLOGY
SCHOOL OF ELECTRICAL ENGINEERING

KTH ROYAL INSTITUTE OF TECHNOLOGY



MASTER THESIS

Thermal Analysis and Control of MIST CubeSat

Author:

Shreyas Chandrashekhar

Supervisor:

Andreas Berggren

Examiner:

Tomas Karlsson

*A thesis submitted in fulfillment of the requirements
for the degree of Master of Science*

in the

Department of Space and Plasma Physics
School of Electrical Engineering

February 8, 2017

Abstract

The thermal analysis and control provides the necessary means to control the temperature of the satellite during the harsh conditions in space. MIST CubeSat presents a challenging task to design such a system with its various payloads and subsystems on board. This thesis report aims to describe the modelling and design of the thermal control system developed for MIST CubeSat in detail.

Each of these payloads and subsystems have different thermal requirements that has to be met in order to maintain thermal equilibrium. Hence in this project, all the units are given equal importance for the analysis to ensure the safety. A detailed thermal model of MIST CubeSat was developed using Systema-Thermica software. With this model, three different thermal cases such as the Hot Operational case, Cold Non-Operational and Operational cases were analysed. Furthermore, an initial dissipation profile for all the units present in the CubeSat was created for the thermal analysis. Based on the temperatures obtained, a thermal control system was designed to maintain the thermal balance between the satellite and the environment. This report also gives details of the assumptions made at certain points of the analysis.

The thermal control system for MIST CubeSat consists of both passive and active means. The passive means includes the use of thermal tapes on some of the payloads and subsystems on board. It was observed that the passive means were not enough to maintain the temperatures and hence active systems such as heaters were implemented for certain units. The results indicate that not all the payloads are within the tolerable limits and hence further development of the thermal control system is needed. Lastly the results include the overall design changes made in the model and a conclusion along with a possibility of future work has been discussed.

Sammanfattning

Termisk analys och kontroll förser de nödvändiga metoderna för att kontrollera temperaturen på satelliten under de extrema omständigheterna i rymden. MIST CubeSat presenterar en utmanande uppgift i att designa ett sådant system med dess olika nyttolaster och delsystem ombord. Denna rapport syftar till att beskriva i detaljerad modellering och designen av den termiska kontrollen som har utvecklats för MIST CubeSat.

Var och en av dessa nyttolaster och delsystem har olika termiska krav som måste uppfyllas för att upprätthålla termisk jämvikt. Därför i detta projekt, alla enheter ges lika stor betydelse för analysen för att kunna garantera dess termiska jämvikt. En detaljerad termisk modell av MIST CubeSat har utvecklats med hjälp av Systema-THERMICA programvara. Med denna modell, tre olika termiska fall har analyserats; Varmt operativt fall, Kallt icke-operativt samt kallt operativa fall. Experimentens och del systemens dissipationsprofil kommer ha betydelse för temperaturen av enheten och en förenklad profil för de olika enheterna har implementerats i denna termiska modell. Baserat på de temperaturer som erhölls, ett termiskt styrssystem var konstruerad för att bibehålla den termiska jämvikten mellan satelliten och omgivning. Denna rapport presenterar också detaljer om de antaganden som gjorts vid vissa moment i analysen.

Det termiska styrssystem för MIST CubeSat består av både passiva och aktiva metoder. Den passiva metoden inkluderar användning av termisk tejp på en del av nyttolasterna och delsystemen ombord. Det kunde konstateras att den passiva metoden inte var tillräckligt för att bibehålla temperaturerna och därmed aktiva system, såsom värmare användas för vissa enheter. Resultaten tyder på att inte alla nyttolaster ligger inom acceptabla gränser och därmed ytterligare utveckling av den termiska styrssystem behövs göras. Slutligen, resultaten inkluderar de övergripande konstruktionsändringar som gjorts i modellen samt en slutsats om möjlighet till framtida arbete har diskuterats.

Acknowledgement

Firstly I would like to express my sincere gratitude to my supervisor Mr.Andreas Berggren for his continuous support and guidance throughout the thesis work. His constant motivation and enthusiasm helped me to complete this work successfully. I could not have imagined having a better advisor and mentor for my thesis.

I am very grateful to my project manager Dr.Sven Grahn for granting me this great opportunity to work under MIST satellite project at KTH and also for his continuous support throughout the work. His professional guidance and expertise gave me great insights on how the real space mission is run.

Furthermore, I would like to thank Mr.Simon Görries for his excellent leadership of the MIST student team and Project Assistant Agnes Gårdebäck for her valuable inputs throughout the work. Also I am very thankful to rest of the team members who were working with me during the semester.

I also would like to thank Prof.Tomas Karlsson for being my thesis examiner and providing me with an overview of thesis work at the initial stages.

Special thanks to my close friends Jiewei Zhou, Oscar Bylund and Rutvika Acharya for their continuous encouragement and fun times during the entire work.

Finally, I must express my very profound gratitude to my parents and to my friends for providing me with unfailing support and courage throughout my years of study and through the process of researching and writing this thesis. This accomplishment would not have been possible without them. Thank you.

Contents

Abstract	ii
Acknowledgement	iv
List of Figures	viii
List of Tables	x
List of Abbreviations	xii
1 Introduction	1
1.1 Aim	1
1.2 Boundaries	2
1.3 Report Outline	2
2 The MIST CubeSat	3
2.1 MIST Mission Characteristics	3
2.2 Satellite Overview	3
2.3 Subsystems	4
2.3.1 Batteries	4
2.3.2 Electrical Power System Board	5
2.3.3 On Board Computer (OBC)	5
2.3.4 Magnetorquer (iMTQ's)	6
2.3.5 TRXVU Transceiver	6
2.3.6 Antenna System	7
2.3.7 Solar Panels	7
2.4 Scientific Payloads	8
2.4.1 CubeProp	8
2.4.2 SEUD	9
2.4.3 MOREBAC	10
2.4.4 RATEX-J	10
2.4.5 SIC	11
2.4.6 CUBES	11
2.4.7 LEGS	12
2.4.8 Camera	13
2.5 CubeSat Structure	13

2.5.1	MIST CubeSat Orientation	14
3	Theory	16
3.1	Conduction	16
3.1.1	Thermal Contact Conductance	17
3.1.2	Conductive Couplings	18
3.2	Radiation	19
3.2.1	Radiative view factors	19
3.2.2	Radiative heat transfer	20
3.3	Space Thermal Environment	20
3.3.1	Solar radiation	21
3.3.2	Earth Albedo	21
3.3.3	Earth IR	22
3.4	Heat Capacity of the material	22
3.5	Transient Heat Equation	23
4	Thermal Modelling of MIST CubeSat	24
4.1	Thermal Model	24
4.1.1	Batteries	25
4.1.2	Electrical Power System (EPS)	26
4.1.3	On Board Computer (OBC)	27
4.1.4	ISIS Magnetorquer Board (iMTQ's)	29
4.1.5	TRXVU Transceiver	30
4.1.6	Antenna system	31
4.1.7	Solar Panels	32
4.1.8	CubeProp	34
4.1.9	SEUD	35
4.1.10	MOREBAC	37
4.1.11	RATEX-J	38
4.1.12	SIC	40
4.1.13	CUBES	41
4.1.14	LEGS	42
4.1.15	Camera	44
5	Thermal Analysis of MIST CubeSat	46
5.1	Thermal Requirements for MIST	46
5.2	Internal Heat Dissipation	48
5.2.1	Operational Case	49
5.2.2	Non-Operational Case	50
5.3	Thermal model analysis	50
5.3.1	Hot Case	50
5.3.2	Cold Case	51
6	Thermal Control Design	52
6.1	Passive Control System	52
6.1.1	First Surface Mirrors	52
6.1.2	Second Surface Mirrors	53

6.2	Active control System	53
6.2.1	Heaters	53
6.3	Analysis results	54
6.3.1	Hot Operational Case :	54
6.3.2	Cold-Non Operational case:	57
6.3.3	Cold Operational Case:	60
6.4	New Thermal Model	61
7	CONCLUSIONS	62
7.1	Conclusion	62
7.2	Future Work	62
A	Geometrical Model Properties	64
A.1	Material Properties	64
A.2	Optical Properties	65
B	Internal Heat Dissipations	67
C	Figures	68
	Bibliography	70

List of Figures

2.1	Structure of MIST [30]	4
2.2	NanoPower BP4 battery pack [3]	5
2.3	NanoPower P31-us [4]	5
2.4	ISIS OBC board [5]	6
2.5	ISIS Magnetorquer Board [6]	6
2.6	ISIS TRXVU Transceiver Board [7]	7
2.7	ISIS deployable antenna system [8]	7
2.8	Body Mounted solar panels [9]	8
2.9	NanoSpace CubeProp Module [CAD Model] [10][28]	9
2.10	Architecture of SEUD Experiment [11]	9
2.11	Crude sketch of the MOREBAC experiment [12]	10
2.12	Model of RATEX-J experiment [13]	10
2.13	Schematic of the Experiment [14]	11
2.14	Layout of the Experiment [15]	12
2.15	LEGS Module [16]	12
2.16	Camera Module [17]	13
2.17	ISIS 3U Modular Structure [18]	13
2.18	The Orbital Frame	14
2.19	Body and Orbital frames in reference orbit	15
3.1	Heat conduction through a large plane wall of thickness Δx and area A.	17
3.2	Thermal contact conductance	17
3.3	Conductive coupling between two nodes	18
3.4	Two differential areas for calculating view factors [31]	19
3.5	The Space environment	21
4.1	MIST Thermal Model	24
4.2	Thermal Model of GomSpace Batteries	25
4.3	Thermal Model of GomSpace power system	27
4.4	Thermal Model of ISIS OBC	28
4.5	Thermal Model of ISIS Magnetorquer board	29
4.6	Thermal Model of ISIS TRXVU- transceiver board	30
4.7	Thermal Model of ISIS antenna system	32
4.8	Thermal Model of ISIS solar panels	33
4.9	Thermal Model of NanoSpace-CubeProp	34
4.10	Thermal Model of SEUD	36

4.11	Thermal Model of MOREBAC	37
4.12	Thermal Model of RATEX-J (Inside View)	38
4.13	Thermal Model of RATEX-J	39
4.14	Thermal Model of SIC	41
4.15	Thermal Model of CUBES	42
4.16	Thermal Model of Piezo-LEGS	43
4.17	Thermal Model of Camera	44
5.1	Trajectory of the MIST	46
5.2	Temperature definitions for Thermal Control System (TCS)	48
5.3	Subsystem-Heat Dissipation Profile	49
5.4	Operational Case-Heat Dissipation Profile	49
6.1	Concept of First Surface Mirror (FSM) [25]	52
6.2	Concept of Second Surface Mirror (SSM) [25]	53
6.3	Typical heaters used for the satellites [26]	53
6.4	Temperature limit plot for Hot Operational Case	54
6.5	Temperature limit plot for Cold Non-Operational Case	57
6.6	Temperature limit plot for Cold Operational Case	60
6.7	New Thermal Model	61
A.1	Materials used for MIST CubeSat	64
A.2	Optical coatings used for MIST CubeSat	65
C.1	Thermal temperatures of MIST CubeSat at time zero for the Hot Operational case	68
C.2	Thermal temperatures of MIST CubeSat at time zero for the Cold Non-Operational case	69
C.3	Thermal temperatures of MIST CubeSat at time zero for the Cold Operational case	69

List of Tables

4.1	Model details for the batteries.	26
4.2	Thermal couplings for the batteries.	26
4.3	Model details for the power system.	27
4.4	Thermal couplings for the power system.	27
4.5	Model details for the OBC.	28
4.6	Thermal couplings for the OBC.	28
4.7	Model details for the Magnetorquers.	29
4.8	Thermal couplings for the Magnetorquers.	30
4.9	Model details for the TRXVU transceiver.	31
4.10	Thermal couplings for the TRXVU transceiver.	31
4.11	Model details for the antenna system.	32
4.12	Thermal couplings for the antenna system.	32
4.13	Model details for the Solar panels.	33
4.14	Thermal couplings for the Solar panels.	33
4.15	Model details for the CubeProp.	34
4.16	Thermal couplings for the CubeProp.	35
4.17	Model details for the SEUD.	36
4.18	Thermal couplings for the SEUD.	36
4.19	Model details for the MOREBAC.	37
4.20	Thermal couplings for the MOREBAC.	38
4.21	Model details for the RATEX-J.	39
4.22	Thermal couplings for the RATEX-J.	40
4.23	Model details for the SIC.	41
4.24	Thermal couplings for the SIC.	41
4.25	Model details for the CUBES.	42
4.26	Thermal couplings for the CUBES.	42
4.27	Model details for the Piezo-LEGS.	43
4.28	Thermal couplings for the CUBES.	44
4.29	Model details for the Camera.	45
4.30	Thermal couplings for the Camera.	45
5.1	Temperature requirements for MIST Components.	47
6.1	Thermal temperatures for Hot Operational Case.	55
6.2	Thermal temperatures for Cold Non Operational Case.	58
6.3	Thermal temperatures for Cold Operational Case.	61

A.1	Material properties used in geometric model. [1]	65
A.2	Optical properties used in geometric model. (BOL Values) [1]	66
B.1	Power dissipation values for payloads during operating & idle conditions. .	67
B.2	Power dissipation values for Subsystems during operating & idle conditions.	67

List of Abbreviations

BOL	Beginning Of Life
CUBES	Cubesat x-ray Background Explorer using Scintillators
EOL	End Of Life
ESA	European Space Agency
IR	Infra Red
ISIS	Innovative Solutions In Space
ICD	Interface Control Document
JUICE	JUpiter ICy moon Explorer
KTH	Kungliga Tekniska Högskolan
MIST	MI尼ature Student saTellite
MOREBAC	Microfluidic Orbital REsuscitation of BACteria
OBC	On Board Computer
PCB	Printed Circuit Board
RATEX-J	RAdiation Test EXperiment for Juice
SEUD	Single Event Upset Detector
SiC	Silicon Carbide

1

Introduction

MIST (MIniature Student SaTellite) is a 3U CubeSat being primarily built by the students of KTH Royal Institute of Technology under the supervision of Dr.Sven Grahn. This project started in late 2014 by the initiative of KTH Space Center. It is the first satellite by KTH and is intended to be launched in the year 2017. The CubeSat has eight payloads of different technical and scientific experiments provided by KTH and Swedish Industries. One of the primary aims of this initiative is to provide the students with a sense of real life projects in the area of space technology.

The payloads within the CubeSat are named accordingly as CubeProp, SEUD, MORE-BAC, RATEX-j, CUBES, SIC, LEGS and finally a Camera. Due to the presence of several payloads, there are many challenges encountered while designing the CubeSat and one among them is the thermal analysis. The environmental factors of the satellite during its mission such as the radiation from Sun, Earth and the influence of sun lit and eclipse side along with the internal heat dissipation from the components inside forms an integral part of the design considerations. Besides the subsystems, each of these payloads have different temperature ranges within which they have to be maintained for functioning properly. Once the satellite is placed in orbit, it undergoes extreme fluctuations in temperatures that can affect this performance. Hence it is very important for the satellite to have a reliable thermal control subsystem to guarantee the thermal requirements in every possible way.

1.1 Aim

The main aim of this thesis is to perform a detailed thermal analysis of the MIST CubeSat through simulations in Systema-Thermica and design a suitable thermal control system based on those simulation results. This thesis work entails the detailed description of the thermal model built and the simulation results for hot and cold cases.

1.2 Boundaries

The current thesis work offers the possibility of exploring ways to design a thermal control subsystem for MIST CubeSat. However, considering the available resources and the time constraints, the thesis work is carried out under certain boundaries that are defined below.

- The thesis work only intends to present the simulation results of one such design of the thermal control system and possible suggestions for further design.
- The thesis work only presents the simulation results of the topic using Thermica software and thus no experimental work will be accomplished.
- The thesis will include only the implementation results for the model built and there will be no validation of results presented.

1.3 Report Outline

This report gives a detailed information about the thermal modelling and control of MIST CubeSat. In Chapter 1, a brief introduction about the topic and aim of this thesis work is described. Chapter 2 gives a detailed description about the MIST satellite along with its components. In Chapter 3, a detailed write up about the thermal mathematical model is explained. Chapter 4 contains the simulation results for the cases analyzed. In Chapter 5, the thermal control aspects for the MIST is discussed. Lastly a conclusion for the analysis and possible recommendations for future work is included along with the appendix and references.

2

The MIST CubeSat

The objective of a thermal study is often to understand the behaviour and performance of a satellite structure. For efficient analysis of any satellite, a thermal engineer must be aware of the intended mission and its characteristics along with the detailed overview of the entire structure of the CubeSat.

2.1 MIST Mission Characteristics

The mission objective of MIST CubeSat is to mainly provide students with hands on experience in satellite design and to demonstrate the scientific experiments in space. MIST is the first mission initiated by KTH with an expected mission life time of one year. One of the reference orbits is defined for the LTDN of 1045 at an altitude between 636.8 - 650.8 Km and an inclination of 97.9430 degrees. Furthermore, it is a sun synchronous orbit where in the ground track repeats every 4 days or 59 revolutions around the Earth [2].

However due to the presence of several payloads and other external factors, the launch will be delayed to early 2018 as of current status.

2.2 Satellite Overview

MIST is a 3U CubeSat with the dimensions of $10 \times 10 \times 30 \text{ cm}^3$. The satellite comprises of both subsystems and the payloads inside the structure. All of these systems will mostly consist of Printed Circuit Boards (PCB) as a base line structure. The various subsystems used in the CubeSat are Batteries, power supply unit, On Board Computer, transceiver, Magnetorquer and finally an antenna system. These subsystems are an essential part of the satellite mainly required for keeping the satellite in orbit.

The several payloads in MIST as mentioned before are CubeProp, SEUD, MOREBAC, RATEX-J, CUBES, SIC, LEGS, and lastly a Camera. A display of the entire satellite without the body mounted solar panels is shown in the Figure 2.1 below. The outer

structure consists of two deployable solar panels at the top and body mounted solar panels on all the sides. The detailed study of these systems together is required in order to model them individually and predict their thermal behaviour for such a mission.

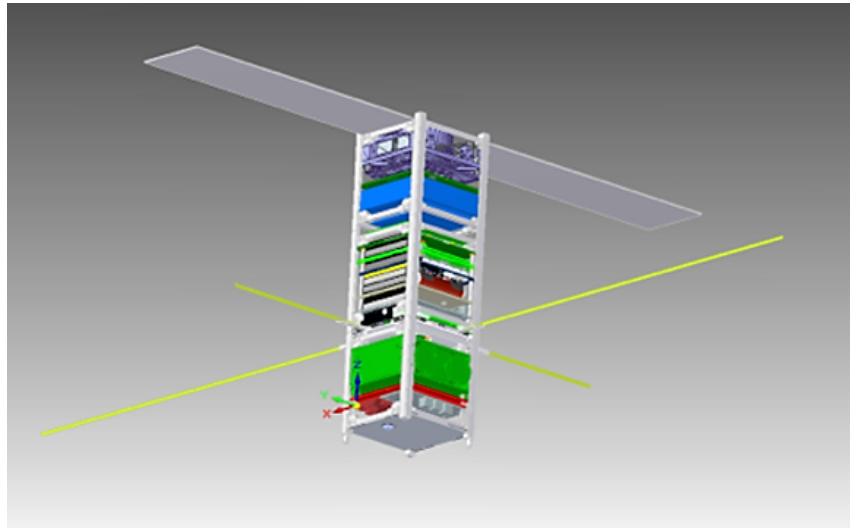


Figure 2.1: Structure of MIST [30]

2.3 Subsystems

The middle stack of the satellite holds the various subsystems required. The entire structure along with these above mentioned subsystems are procured from ISIS (Innovative Solutions In Space) based in The Netherlands. All these components are off the shelf and are readily available from ISIS. The components follow PC104 standards and have specific dimensions in relation with the CubeSat structure built by ISIS.

2.3.1 Batteries

Batteries are generally used on board the satellites to make sure it meets the power requirements during the detumbling and eclipse phases of the orbit. They help in storing, regulating and distributing the necessary power required to complete the mission without any hazard. The batteries used for space applications are generally rechargeable ones. MIST intends to use NanoPower BP4 battery pack from GomSpace which is shown in Figure 2.2. There are four lithium ion cells attached to the PCB which are repacked with some insulation material such as kapton and glued with aluminium brackets for mechanical and thermal stability. These batteries also have built in heaters and temperature sensors to regulate the thermal constraints in space [3]. Although batteries can operate over wide temperature ranges, care must be taken during charging and discharging process. With regard to thermal design of the satellite, batteries are known to be the most sensitive and critical component.



Figure 2.2: NanoPower BP4 battery pack [3]

2.3.2 Electrical Power System Board

The Electrical Power System (EPS) board used in MIST is Nanopower P31-us from GomSpace which is specially designed for small, low cost satellites with power demands from 1 - 30 W [4]. It acts as a power converter to condition the output power from solar panels to charge the provided lithium-ion batteries.



Figure 2.3: NanoPower P31-us [4]

Figure 2.3 shows the EPS board currently used for MIST and is considered to be an important unit that has to be thermally stable.

2.3.3 On Board Computer (OBC)

The On Board Computer used for MIST is from ISIS which is intended for space applications. It provides powerful computing functions by running specialized software to control and manage the operations of the satellite [5]. It helps in the communication between the On-board subsystems and ground station. When the ground station is not in reach, OBC takes over the control of all critical operations on board. Figure 2.4 shows the OBC board along with the daughter board used. Having broader temperature ranges, this subsystem is unlikely to be any kind of concern for the thermal analysis.



Figure 2.4: ISIS OBC board [5]

2.3.4 Magnetorquer (iMTQ's)

The attitude and determination control system for MIST comprises of the magnetorquer alone since it is a magnetically controlled satellite. It is solely responsible for keeping the CubeSat dynamically stable. The magnetorquer is again procured from ISIS which is specifically designed for CubeSat applications.



Figure 2.5: ISIS Magnetorquer Board [6]

This magnetorquer is equipped with internal 3-axis magnetometer, 3 magnetorquers and a micro-controller as shown in Figure 2.5. The power dissipation is upto 1.2 W and the broader temperature qualifications for this board makes it a thermally stable component compared to batteries [6].

2.3.5 TRXVU Transceiver

The ISIS TRXVU is a CubeSat standard compatible transceiver module used by MIST for communication purposes. The module is as shown in Figure 2.6. It performs the function of both transmitter and receiver at appropriate frequencies. This has the highest power dissipation of 4.0 W compared to the other subsystems [7]. However this power is only consumed during transmission and after which it changes to idle mode when inactive.



Figure 2.6: ISIS TRXVU Transceiver Board [7]

The thermal connections between this module and the structure should be properly provided in order to avoid any over heating of the components.

2.3.6 Antenna System

The ISIS deployable antenna system used for MIST consists of four memory alloy tape antennas up to 55 cm length which can deploy from all four sides of the structure upon command [8]. The main purpose of this antenna system is to deploy the stowed antennas so that it can be used for RF transmissions.

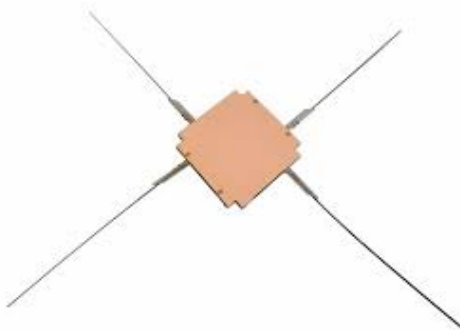


Figure 2.7: ISIS deployable antenna system [8]

This antenna system has a thermal mass of 100 gms and has a broader temperature requirements. Figure 2.7 shows the exact model that will be used for the MIST CubeSat.

2.3.7 Solar Panels

The solar panels are on board the satellite for power supply. There are two deployable solar panels at the top of the satellite and the rest of the solar panels are mounted on each

side of the CubeSat. Both the deployable and body mounted solar panels are designed in such a way that it is in interface with the CubeSat electrical power system (EPS) and On board Computer (OBC) [9]. Figure 2.8 shows the solar cells and the body mounted solar panels for a dummy structure. The solar cells employed are used generally for space applications and hence they can withstand higher temperatures. The deployable solar panels are hinged at the top of the CubeSat structure and are deployed after detumbling process in space.

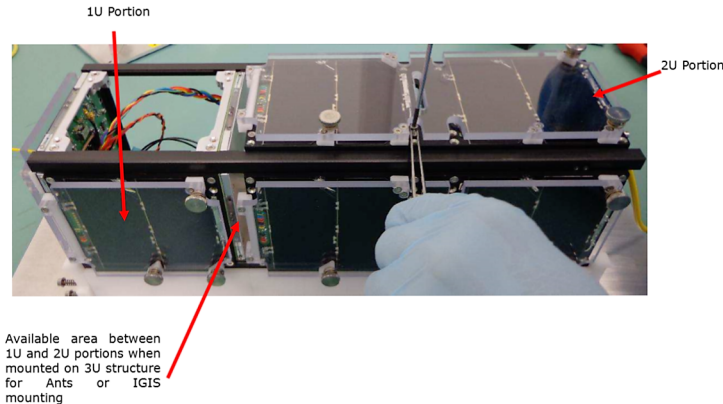


Figure 2.8: Body Mounted solar panels [9]

2.4 Scientific Payloads

The upper and the lower stack of the CubeSat holds the various payloads that are provided by the experimenters. There are eight payloads that will be carried to space for various scientific experiments. A detailed overview of these payloads will be discussed in this section since it plays an important role in the thermal design.

2.4.1 CubeProp

CubeProp is the propulsion module from Nanospace company in Uppsala, Sweden. It is half the unit (0.5 U) in size and is as shown in Figure 2.9. The purpose of this experiment is to get a flight heritage for this module so that it can be used specifically for CubeSat applications in the future. The goal will be to use the propulsion system in such a way that precision control of the satellite can be demonstrated and also to test the total impulse capability of the system to be around 40 Ns [10]. The module consists mainly of thrusters, propellant tank, valves, filters and electronic boards. The main concern from the thermal standpoint is the propellant tank where in the fuel used is butane.

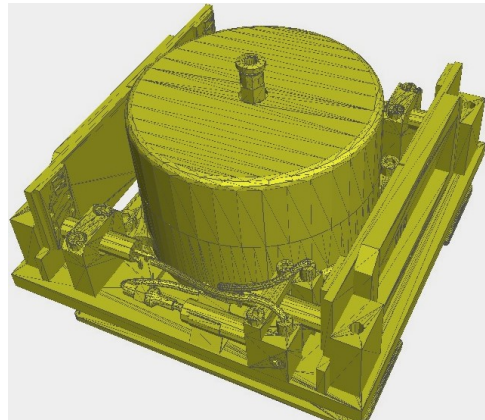


Figure 2.9: NanoSpace CubeProp Module [CAD Model] [10][28]

The tank has to be thermally controlled within the required temperatures such that it does not over heat or freeze the fuel during the mission. Hence the CubeProp is an important payload and is one of the critical units in MIST that has to be maintained.

2.4.2 SEUD

SEUD stands for Single Event Upset Detector which is developed by KTH. The purpose of the experiment is twofold, one is to test the in house concept of self healing computer system in space to see if it will be able to heal itself by correcting faults during run time. The second purpose is to measure the expected SEU frequency in near Earth orbit. The payload is intended to be a simple FPGA (field-programmable gate array) board and the experiment layout is as shown in Figure 2.10.

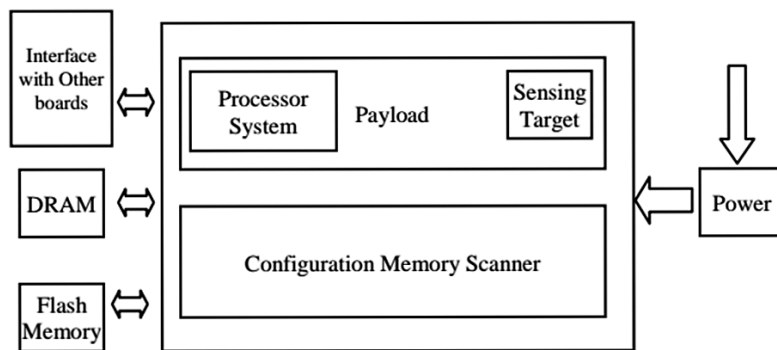


Figure 2.10: Architecture of SEUD Experiment [11]

This experiment is unlikely to be considered as a critical unit in terms of thermal conditions, nevertheless it has to be within the limits. The temperature requirements for this unit is much wider than compared to others and also has a bit higher power dissipation of upto 1.2 W [11].

2.4.3 MOREBAC

MOREBAC stands for Microfluidic Orbital Resuscitation of Bacteria is an experiment that is proposed by the Division of Proteomics and Nanobiotechnology, KTH. The main aim of this payload is to transport freeze dried micro-organisms into orbit, resuscitate them through media addition and finally measure their growth characteristics in orbit after a certain storage period [12]. The experiment is still in its development stage and hence only the sketch of the experiment is available as of now which is as shown in Figure 2.11. This experiment is also one of the most critical unit because of its narrow temperature demands. The bacteria can only sustain within the thermal limits for this experiment to work. Therefore this unit is expected to be the driving factor for thermal design and control.

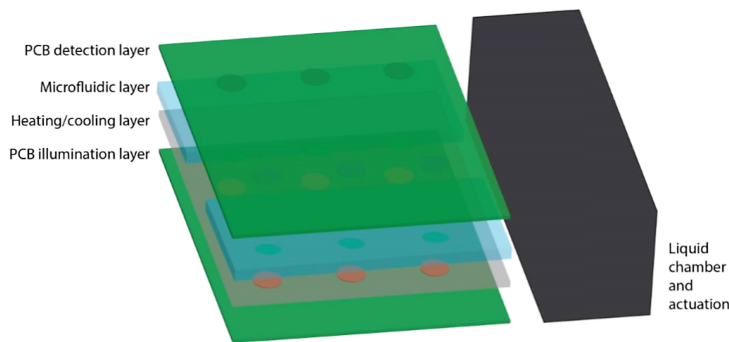


Figure 2.11: Crude sketch of the MOREBAC experiment [12]

2.4.4 RATEX-J

RATEX-J stands for RAdiation Test EXperiment for Juice mission proposed by Swedish institute of space physics in Kiruna, Sweden. It is a prototype which consists of three different detectors to be implemented in the JDC (Jovian plasma Dynamics and Composition) instrument for ESA's Jupiter Icy Moon Explorer (JUICE) mission. The initial model of the experiment is as shown in Figure 2.12.

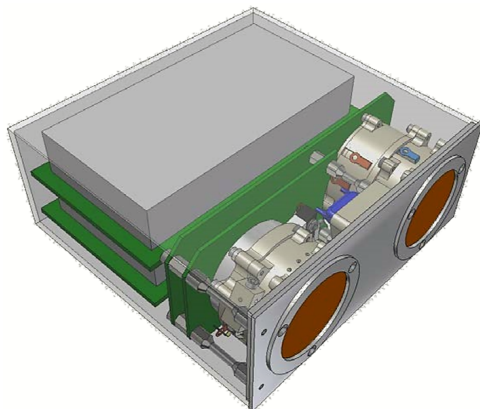


Figure 2.12: Model of RATEX-J experiment [13]

The three different particle detectors are Solid State Detector (SSD) , Multi-Channel Plate (MCP) and Ceramic Channel Electron Multiplier (CCEM) [13]. This experiment is exposed continuously towards space for the experiment to be successful and therefore the side which has detectors does not have any body mounted solar panels covering them.

2.4.5 SIC

The SiC (Silicon Carbide) experiment is intended to study the silicon carbide material in harsh space conditions for future use in electronics. This application has also been already suggested for a Venus lander mission [14]. The payload consists of a SiC transistor, a Graphene transistor and a Silicon transistor on simple PCB. Through the MIST mission, it is being tested for in orbit low TRL (Technology Readiness Level) technologies.

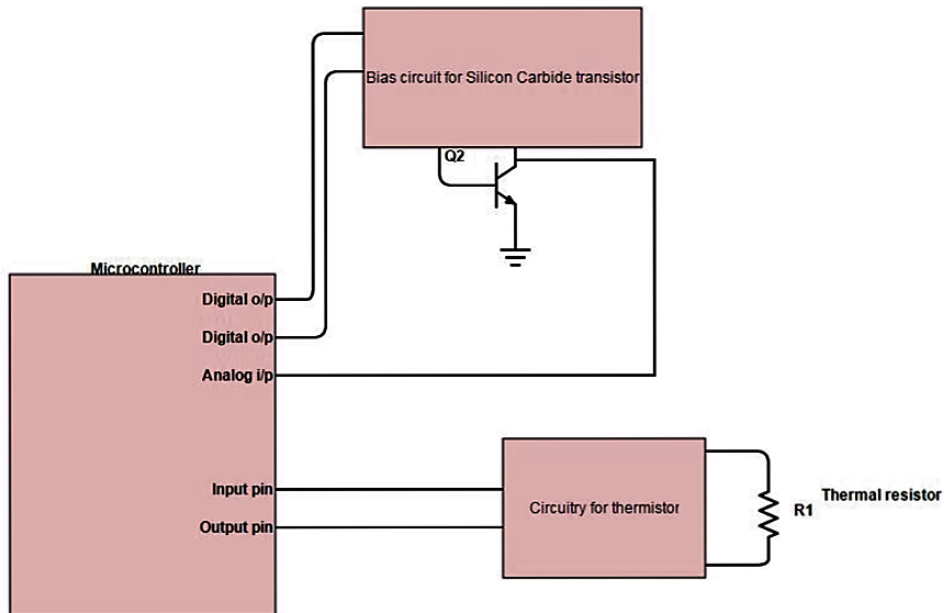


Figure 2.13: Schematic of the Experiment [14]

From the thermal standpoint, this payload is unlikely to be considered as critical because of its broader temperature range. Since this experiment is still in its development phase, only the schematic of the experiment is shown in the Figure 2.13.

2.4.6 CUBES

CUBES stands for CUBesat x-ray Background Explorer using Scintillators is an experiment proposed by Particle and Astroparticle Physics group at KTH. The main purpose of this experiment is to study the in orbit radiation environment using a detector comprising a silicon photomultiplier coupled to scintillator material. The studies will focus on possible radio-activation, induced fluorescence and radiation damage for the scintillator

materials [15]. This experiment has very narrow temperature range within which it has to be maintained and also the scintillators should be exposed to space all the time. This is also an important payload to be considered for thermal design. The overview of the experiment is shown in Figure 2.14.

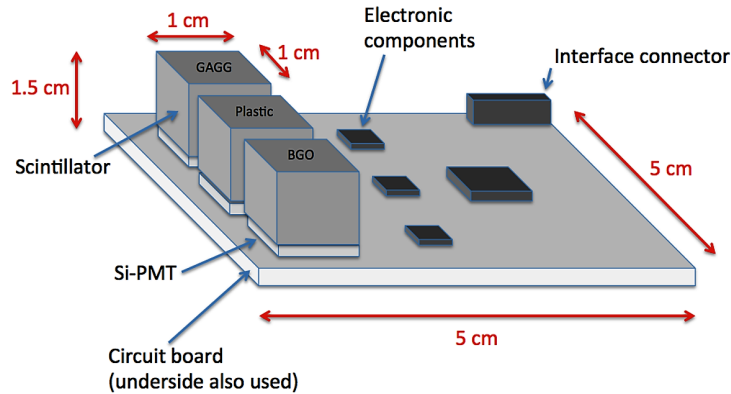


Figure 2.14: Layout of the Experiment [15]

2.4.7 LEGS

The piezo LEGS experiment is proposed by the company Piezomotor AB in Uppsala, Sweden. The aim of this experiment is to test the piezomotor applications in space. It is of interest to observe that the motor works in the vacuum filled radiation environment. Finally the test will be to observe the motors function over time (several months) to check for possible change of performance and the distance the motor can work [16].

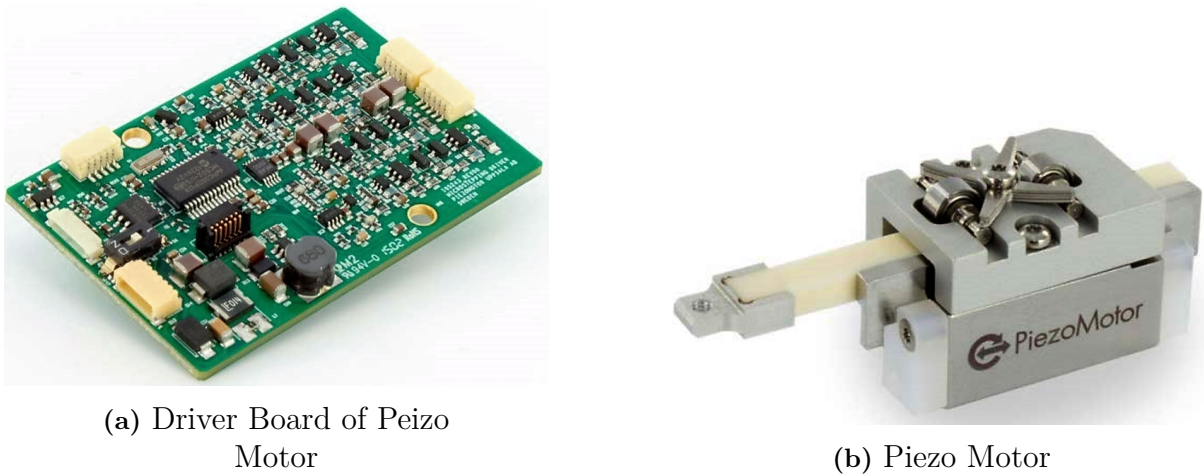


Figure 2.15: LEGS Module [16]

The payload consists of the driver board and the piezo motor as shown in Figure 2.15a and 2.15b . The thermal conditions required are feasible but since the experiment is positioned with CUBES experiment, it is also exposed to space continuously.

2.4.8 Camera

The camera intended to be used in MIST is Raspberry Pi camera as of now. The goal of this experiment is to capture and reconstruct high quality images from MIST. The images will be captured using High Dynamic Range (HDR) techniques, compressed using a new learning based compression method adapting to the input data, and processed using compressive image reconstruction techniques [17]. The final images of the camera will be displayed at Tekniska Museet in Stockholm. The camera module of the MIST is situated at the lower stack and is facing the Earth (Nadir pointing). Thermal management of this payload is also equally important as a whole. Figure 2.16 shows the currently considered Raspberry Pi camera module connected to Raspberry Pi.



Figure 2.16: Camera Module [17]

2.5 CubeSat Structure

MIST intends to use the ISIS modular structure which is of the CubeSat standards. The ISIS CubeSat STS (STructural Subsystem) is built in such a way that the PCBs can be mounted on to a set of four ribs. These structural ribs interface with side frames. Figure 2.17 shows the intended MIST structure delivered by ISIS.



Figure 2.17: ISIS 3U Modular Structure [18]

The rails on the outside are black anodized painted to have absorptivity to emissivity

ratio equal to 1 for a better thermal stability [18]. The structure is according to CubeSat standards and hence it must withstand the harsh temperature conditions in space.

2.5.1 MIST CubeSat Orientation

The CubeSat's direction of orientation and the coordinate frames are very important for a thermal engineer as it is to an attitude control engineer. The direction of travel for the CubeSat will determine which face of the satellite is experiencing maximum and minimum solar exposure. Along with the direction of travel, it is also important to know the placements of payloads within the CubeSat which are placed according to the criteria required for the experiment. The orbital frame (U,V,W) is defined as follows :

- U is along the direction of the radius vector (Zenith) from the Earth's center to the satellite.
- V is perpendicular to U and points in the general direction of orbital motion.
- W is perpendicular to the orbital plane and completes the coordinate system. Figure 2.18 shows the orbital frame of reference stated.

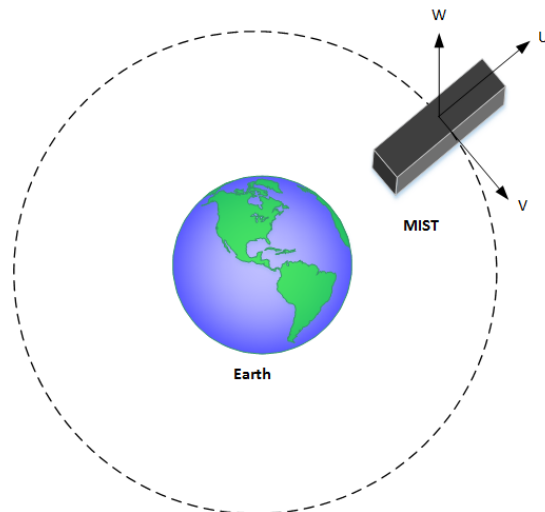


Figure 2.18: The Orbital Frame

The particle detector experiments like the RATEX-J and the CUBES need to be placed in the dark side of the satellite where there is minimum exposure to the Sun. Hence these particle detectors are placed in -X direction which point in -W direction of the orbital plane in a Sun synchronous orbit specified earlier. With regard to the Camera, it is always facing the Earth and hence is placed on the -Z face (Nadir pointing) and this is pointing in the -U direction of the orbital plane. Lastly, it is observed that -Y direction is aligned with the +V direction. Figure 2.19 shows the orientation of body and orbital frames in the reference orbit described in section 3.1.

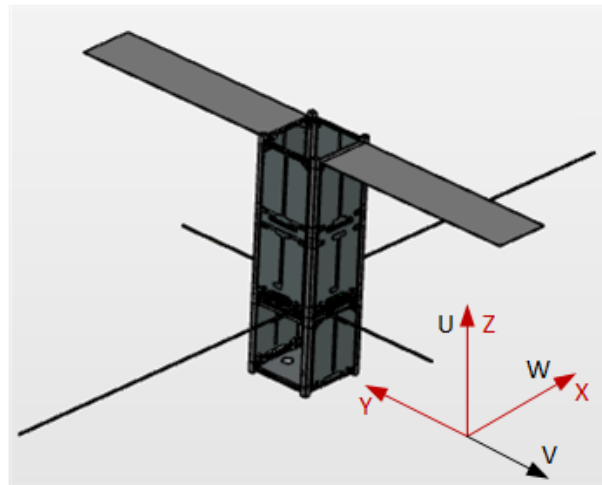


Figure 2.19: Body and Orbital frames in reference orbit

Since the experiments like RATEX-J and CUBES are facing the -X direction and cannot be shadowed by the deployable solar panels, they are made to be deployed from the Y faces and are pointing towards +Z direction of the CubeSat. In addition to this, the experiments have to be exposed to space and hence there is no body mounted solar panel in the -X direction of the lower stack. The orientation of the antennas from the work by Bsc. thesis students of MIST shows that the shorter element of the antenna should be along the \pm Y direction and the longer elements should be along the \pm X direction [19].

3

Theory

Transfer of energy is one of the basic phenomena that is observed everywhere in the universe. Heat is a form of this energy that can be transferred from one system to another system as a result of temperature difference. There are three modes of heat transfer mechanisms [22] that are usually observed such as

- Conduction
- Convection
- Radiation

Conductive and radiative heat transfer are the main modes of transfer mechanisms within a spacecraft in space. Convection is not generally observed in space because all the components of the spacecraft are in vacuum. Each of these phenomena are discussed except for convection as to how they affect the spacecraft in those harsh conditions of space.

3.1 Conduction

Conduction is defined as the transfer of energy from the more energetic particles of a substance to the adjacent less energetic particles as a result of interactions between the particles. The rate of heat conduction through the medium depends on geometry of the medium, thickness, material of the medium and finally the temperature difference across the medium.

Consider a steady state conduction through a large plane wall of thickness $\Delta x = L$ and the temperature difference across the wall is $\Delta T = T_2 - T_1$ as shown in the Figure 3.1. The rate of heat conduction through a plane layer is proportional to the temperature difference across the layer and heat transfer area but is inversely proportional to the thickness of the layer.

$$\dot{Q} = \frac{KA(T_1 - T_2)}{\Delta x} = -KA\frac{\Delta T}{\Delta x} = -KA\frac{dT}{dx} \quad (W) \quad (3.1)$$

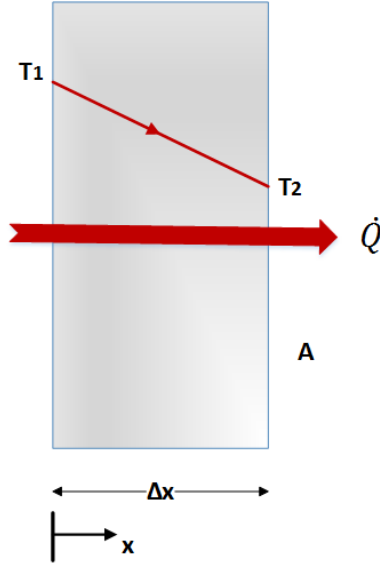


Figure 3.1: Heat conduction through a large plane wall of thickness Δx and area A .

where K is thermal conductivity in $\frac{W}{mK}$ and A is cross-sectional area of the surface in m^2 . Now this is called the Fourier's law of heat conduction. The relation 3.1 indicates that the rate of heat conduction in a direction is proportional to the temperature gradient in that direction. The negative sign ensures that the heat transfer in the positive x direction is a positive quantity.

3.1.1 Thermal Contact Conductance

This is a property where it describes the ability to conduct heat flow between two bodies. Consider two bodies A_1 and A_2 in contact where heat flows from the hotter body to the colder body as shown in Figure 3.2. Now the heat flow observed between the two bodies A_1 and A_2 can be obtained from the Equation 3.2 :

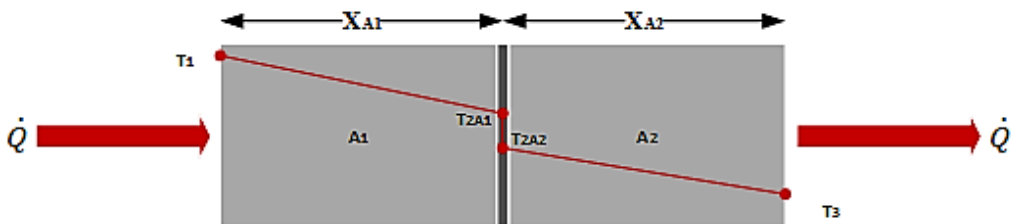


Figure 3.2: Thermal contact conductance

$$\dot{Q} = \frac{(T_1 - T_3)}{\frac{\Delta X_{A_1}}{K_{A_1} A} + \frac{1}{h_c A} + \frac{\Delta X_{A_2}}{K_{A_2} A}} \quad (W) \quad (3.2)$$

where T_1 and T_3 are the temperatures at the end of each bodies and ΔX_{A_1} ΔX_{A_2} are the distances through which the heat has conducted. Also h_c is the thermal contact conductance and A is the contact area.

3.1.2 Conductive Couplings

While performing the thermal analysis, the CubeSat is discretized into several number of nodes for each of the parts modelled. These nodes in turn have conductive heat transfer between them that is taken into account. The conductive heat transfer between two surfaces in contact form a coupling. For example, consider two surfaces A_1 and A_2 in contact with each other where in the nodes are present at the centre of each surface as shown in the Figure 3.3. The conductive coupling between two nodes can be obtained from the Equation 3.1 as follows :

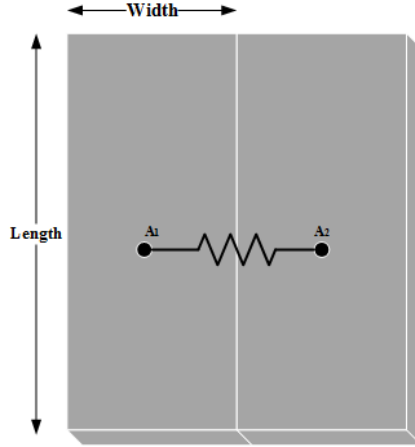


Figure 3.3: Conductive coupling between two nodes

$$G_{A_1/A_2} = \left(\frac{KA}{dx} \right)_{A_1/A_2} \quad (W/K) \quad (3.3)$$

$$GL_{A_1 \rightarrow A_2} = \frac{1}{\frac{1}{G_{A_1}} + \frac{1}{G_{A_2}}} \quad (W/K) \quad (3.4)$$

where G_{A_1/A_2} is the conductance of node A_1 or node A_2 and dx is the distance traversed by the heat. The $GL_{A_1 \rightarrow A_2}$ denotes conductive coupling between the two nodes as represented in the Figure 3.3. The value of this thermal conductance depends on the material of the surface, contact pressure between the surfaces, size of the area in contact, surface cleanliness and roughness of the material. The various conductive couplings present in the thermal model are fed in manually for Systema-Thermica software to aid in the calculation of temperatures.

3.2 Radiation

Radiation is the energy emitted by matter in the form of electromagnetic waves (or photons) as a result of the changes in the electronic configurations of the atoms or molecules. In case of heat transfers due to this phenomenon, all bodies above absolute zero emit thermal radiation. The radiative heat transfer from a black body surface is given by the Stefan-Boltzmann law as :

$$\dot{Q}_{max} = \sigma AT^4 \quad (W) \quad (3.5)$$

where $\sigma = 5.67 * 10^{-8} W/m^2 K^4$ is the Stefan Boltzmann constant, A is the area of the surface in m^2 and T is the temperature in K [20]. However this is an ideal case for a black body. The radiative heat transfer from the real surfaces is less than the radiation emitted by black body and is expressed as :

$$\dot{Q}_{emit} = \epsilon \sigma AT^4 \quad (W) \quad (3.6)$$

where ϵ is the emissivity of the surface. This property is defined as the ratio between energy that the gray body emits to the energy emission it would have if it were a black body. Another important property of the surface is known as absorptivity denoted by α which is the fraction of the radiation energy incident on a surface that is absorbed by the surface.

3.2.1 Radiative view factors

The radiative heat exchange depends on the orientation of the two surfaces relative to each other. The view factor also known as shape factor is the one which describes this orientation.

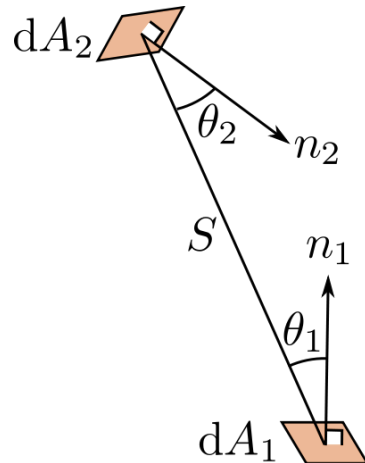


Figure 3.4: Two differential areas for calculating view factors [31]

3. Theory

Consider two surfaces having differential areas dA_1 and dA_2 as shown in the Figure 3.4. The distance between the two surfaces is S and the angles between the surface normals (n_1 and n_2) and the line S is θ_1 and θ_2 respectively. The differential view factor $dF_{dA_1 \rightarrow dA_2}$ is given by the expression as

$$dF_{dA_1 \rightarrow dA_2} = \frac{\cos\theta_1 \cos\theta_2}{\pi S^2} dA_2 \quad (3.7)$$

The exact solution for the above equation after solving can be finally written as

$$F_{A_1 \rightarrow A_2} = \frac{1}{A_1} \int_{A_1} \int_{A_2} \frac{\cos\theta_1 \cos\theta_2}{\pi S^2} dA_2 dA_1 \quad (3.8)$$

Equation 3.8 accounts for the effects of orientation on radiative heat transfer between two surfaces. It is an independent quantity which is purely geometrical and does not depend on temperature.

3.2.2 Radiative heat transfer

The radiative heat transfer between two nodes A_1 and A_2 within the spacecraft can be expressed as follows :

$$\dot{Q}_{A_1 \rightarrow A_2} = GR_{A_1 \rightarrow A_2} \sigma (T_{A_1}^4 - T_{A_2}^4) \quad (W) \quad (3.9)$$

where $\dot{Q}_{A_1 \rightarrow A_2}$ is the heat flow from node A_1 to A_2 , $GR_{A_1 \rightarrow A_2}$ is the radiative coupling (also known as Radiative Exchange Factor (REF)) in W/K^4 between those two nodes and T_{A_1} and T_{A_2} are temperatures in node A_1 and A_2 respectively. Now the radiative coupling is expressed as :

$$GR_{A_1 \rightarrow A_2} = \epsilon_{A_1} B_{A_1 \rightarrow A_2} A_{A_1} \quad (3.10)$$

where ϵ_{A_1} is the emissivity of node A_1 , $B_{A_1 \rightarrow A_2}$ is the Gebhart factor from node A_1 to A_2 and A_{A_1} is the area of that node. Now the Gebhart factor can be calculated from the expression shown in Equation 3.11

$$B_{A_1 \rightarrow A_2} = F_{A_1 \rightarrow A_2} * \epsilon_{A_2} + \sum_{j=1}^N ((1 - \epsilon_{A_j} * F_{A_1 j} * B_{j A_2})) \quad (3.11)$$

where $F_{A_1 \rightarrow A_2}$ is the radiative view factor discussed in section 3.2.1 and ϵ_{A_2} is the emissivity of node A_2 . The radiative couplings along with the view factors and Gebhart factors are calculated automatically by Systema-Thermica with the use of Monte Carlo Ray Tracing method and is later supplied to the Thermisol solver for temperature calculations.

3.3 Space Thermal Environment

The environment for the spacecraft play an important role in the thermal management system. The main sources for the imbalance of the thermal system of the spacecraft are

due to solar radiation, Earth Albedo and Earth IR. The temperature surrounding the satellite in space is 2.7K and thus serves as the harsh environment [1]. Figure 3.5 shows the main sources of heat in space.

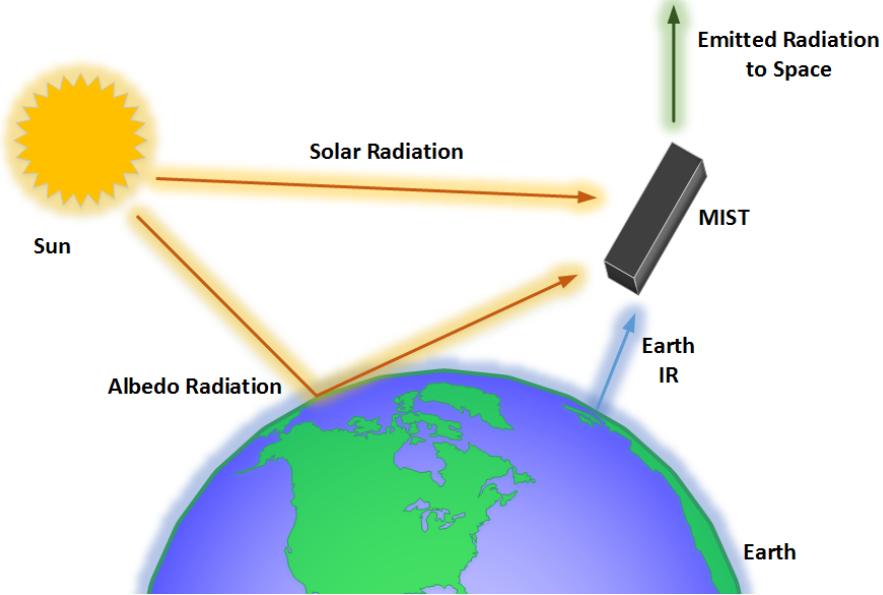


Figure 3.5: The Space environment

3.3.1 Solar radiation

Sunlight is a major source of heating that takes place on the satellite. The way in which it affects the spacecraft depends on the distance from the Sun. During summer solstice, the Earth is farthest from the Sun and it receives low intensity of solar radiation up to 1322 W/m^2 but during winter solstice, the Earth is closest to the Sun and hence the intensity is very high up to 1414 W/m^2 [21]. This is because of the elliptical orbit of the Earth. Heat transferred due to this is given by :

$$\dot{Q}_{A_1,solar} = \alpha_{A_1} S_{solar} A_{A_1} \quad (W) \quad (3.12)$$

where $\dot{Q}_{A_1,solar}$ is the heat input from the solar radiation to the node A_1 , α_{A_1} is the absorptivity of the node A_1 , S_{solar} is the solar flux constant in W/m^2 which is defined as the amount of incoming solar radiation per unit area that would be incident on a plane perpendicular to the rays, at a distance of one astronomical unit (AU) and A_{A_1} is the area of the node perpendicular to the Sun.

3.3.2 Earth Albedo

Sunlight reflecting off the Earth or any planet for that matter is called Albedo. It is actually the fraction of the incident sunlight that is reflected off the surface of the Earth.

Usually the reflectivity is greater over continental regions than oceanic regions and generally increases with decreasing local solar elevation angle and increasing cloud coverage. So in the presence of snow and ice coverage, decreasing solar elevation angle, increasing cloud coverage, Albedo also tends to increase with latitude. As the spacecraft moves away from the sub solar point, the albedo flux reaching the spacecraft decreases. The heat transferred due to Albedo radiation is expressed as :

$$\dot{Q}_{A_1, \text{Albedo}} = \alpha_{A_1} S_{\text{solar}} a A_{A_1} \frac{R_{\text{Earth}}}{(R_{\text{Earth}} + h)^2} \quad (\text{W}) \quad (3.13)$$

where $\dot{Q}_{A_1, \text{Albedo}}$ is the heat input from the Albedo radiation, a is the dimensionless Albedo constant, R_{Earth} is the radius of the Earth and h is the altitude of the spacecraft. The average albedo observed is around 30% [1].

3.3.3 Earth IR

All the incident light on the Earth's surface not reflected as Albedo is absorbed by Earth and eventually re-emitted to space. This re-emitted energy is known as Earth IR. The intensity depends on the local temperature of Earth's surface and also the cloud coverage. At regions of warmer temperatures, the intensity of IR from Earth is higher but at regions of lower temperatures, the intensity is lower. Also it depends on the cloud coverage. In the warmer regions with more cloud coverage, the intensity is again low because of the blocking due to clouds. The heat transferred due to Earth IR is as follows :

$$\dot{Q}_{A_1, \text{Earth-IR}} = \epsilon_{A_1} S_{\text{Earth-IR}} A_{A_1} \frac{R_{\text{Earth}}}{(R_{\text{Earth}} + h)^2} \quad (\text{W}) \quad (3.14)$$

where the ϵ_{A_1} is the emissivity of the node A_1 , $S_{\text{Earth-IR}}$ is the Earth IR flux in W/m^2 . The average value observed for Earth IR is $236 \text{ W}/\text{m}^2$ [1].

3.4 Heat Capacity of the material

Heat Capacity is basically defined as the ratio of the heat added or removed from the object or material to the resulting change in temperature. The relation shows how the thermal capacity for any material is calculated :

$$C = \frac{Q}{\Delta T} \quad (\text{J/K}) \quad (3.15)$$

where C is heat capacity, Q is the heat loss and ΔT is change in temperature. Now for a specific node A_1 with density ρ_{A_1} (kg/m^3), volume V_{A_1} (m^3) and specific heat c_{sp} (J/kgK), the heat capacity can be calculated as shown :

$$C_{A_1} = c_{sp}\rho_{A_1}V_{A_1} \quad (J/K) \quad (3.16)$$

The temperature is dependent on this quantity wherein the temperature change decreases if the heat capacity is higher.

3.5 Transient Heat Equation

The thermal analysis for a spacecraft is generally considered to be a transient process since the concept of heat going in is equal to heat leaving the system is not always true. The transient analysis accounts for the heat storage in the spacecraft as well. Hence the thermal energy balance equation [20] can be written as :

$$C_i \frac{dT_i}{dt} = \dot{Q}_{int,i} + \dot{Q}_{ext,i} - \sum_{i,j}^N GL_{i,j}(T_i - T_j) - \sum_{i,j}^N GR_{i,j}\sigma(T_i^4 - T_j^4) \quad (3.17)$$

Equation 3.17 refers to generic nodes i, j in a N-node discretized spacecraft where in $i, j = A_1, A_2, A_3...etc.$ and it includes all the heat inputs experienced by a spacecraft. On the left hand side, there is the heat input due to thermal capacity whereas on the right hand side, there is the internal heat dissipation from the various components. The external heat inputs are the radiation factors in the environment and finally the heat transfers due to conductive and radiative couplings.

4

Thermal Modelling of MIST CubeSat

This chapter deals with the development of thermal model for MIST CubeSat which will later be simulated to study the thermal behaviour of the MIST during its mission. The entire modelling and simulation is performed with the use of Systema Thermica software which is developed by Airbus Defence and Space [24]. In this process, there are two types of models built, one is the Geometrical Model Management (GMM) and second is the Thermal Model Management (TMM). The GMM includes the geometrical build up of the model MIST in Thermica along with the meshing of geometry into nodes. The TMM however includes the mathematical description of capacitances and conductive couplings for each of the nodes along with dissipation profile for each of the components in MIST.

4.1 Thermal Model

The thermal model of the satellite contains the detailed description about the geometry of MIST CubeSat, materials and optical properties for each of the components used and the thermal couplings between those components.

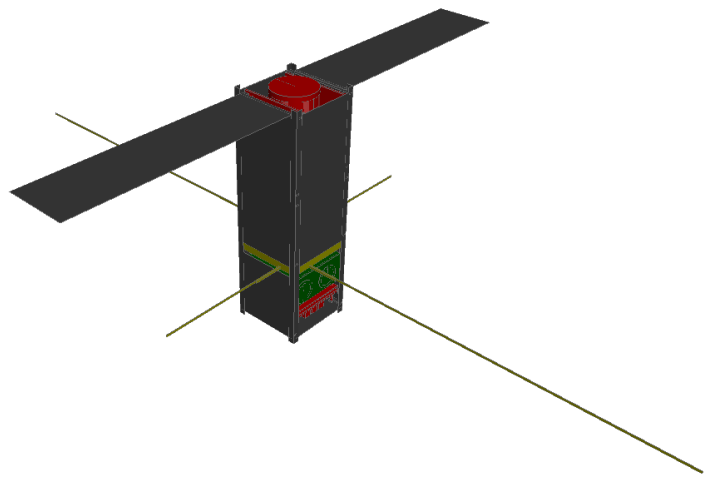


Figure 4.1: MIST Thermal Model

The thermal model of the complete MIST CubeSat is as shown in Figure 4.1. This model consists of all the subsystems and payloads present within the MIST CubeSat and each of these systems are discussed in detail. Note that the mesh geometries used are mostly square plate mesh for PCBs, mounting boards and other box shaped structures whereas the connection stack is meshed as rectangular surface with some thickness. Other mesh geometries include cylinders and discs shaped structures only. Most of the materials used in all the models are assumed accordingly as the information regarding them was still not available when this work was done. All the parts are modelled in such a way that the surfaces are exactly in touch with each other as defined in the original design.

The PCBs make up most of the CubeSat and hence the thermal properties are very important when considered. A PCB is generally made up of alternating layers of copper and that of FR4 which act as the insulation. For the MIST CubeSat, eight layers of copper with 50 % of it on outer layers and 40 % of it on the inner layers has been considered. Also the total thickness of the PCB is taken as 1.6 mm with the calculated average thermal conductivity of 20.5 W/mK . Lastly the average density of 2223 Kg/m^3 and specific heat of 589 J/KgK has been calculated with the same principle from thermal conductivity calculator which was developed in the previous work on thermal analysis by Andreas Berggren [23].

4.1.1 Batteries

There are four battery cells which are cylindrical in shape modelled on the PCB along with a connection stack as shown in Figure 4.2. The thermal couplings observed for this battery is between the cells and PCB, connection stack and PCB and finally PCB with the structure rods. The coupling between the PCB and battery cells includes the coupling of thermal strap which is the main reason for giving mechanical stability to the system. This thermal strap is not geometrically modelled but mathematically considered in the calculations of couplings. The materials used for the batteries along with the capacitances obtained can be seen in the Table 4.1.

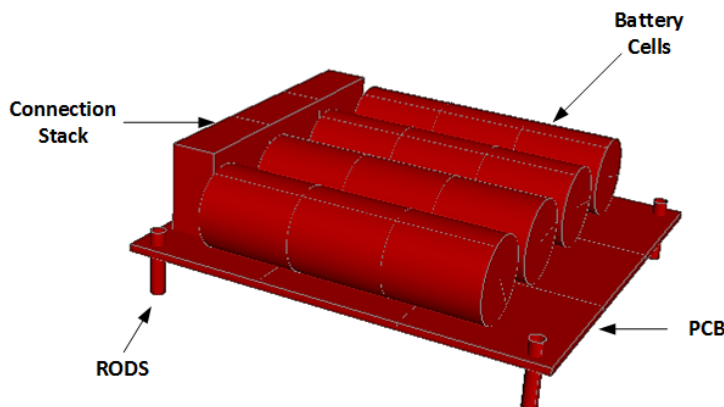


Figure 4.2: Thermal Model of GomSpace Batteries

Table 4.1: Model details for the batteries.

Name of the parts	Material used	Number of nodes	Capacitance per node (J/K)
4 Battery cells	Aluminum 6082	cyl. nodes = 12 disc nodes = 8	cyl. node = 5 disc node = 1
PCB	Copper	9	2
Connection stack	Copper	3	5

The optical coating used for battery cells is Kapton 0.5 mil as mentioned in the interface documents. The PCB has FR-4 coating whereas the connection stack is of copper itself. The conductance coupling between the mentioned parts are shown in Table 4.2. The values for the conductances represent for one element under consideration.

Table 4.2: Thermal couplings for the batteries.

Part 1	Part 2	Conductance (W/K)
Battery cells	PCB	2
PCB	Connection stack	0.4
PCB	Rods	0.1

4.1.2 Electrical Power System (EPS)

The NanoPower P31-us from GomSpace is modelled as a flat PCB with connection stack and small boxes representing the parts of the PCB. The thermal couplings observed are between PCB and the connection stack, PCB with the other boxes and PCB with the structure rods as well. These small boxes are nothing but the electrical units/components part of the PCB. Figure 4.3 shows the thermal model of the NanoPower P31-us built in thermica.

Table 4.3 presents the specific materials used along with their capacitances. The optical properties for each of these surfaces are same as the materials used and no special coating is required for this subsystem. The thermal coupling obtained is presented in Table 4.4.

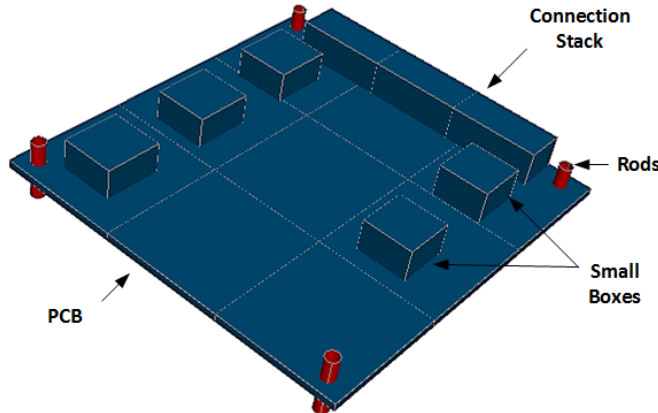


Figure 4.3: Thermal Model of GomSpace power system

Table 4.3: Model details for the power system.

Name of the parts	Material used	Number of nodes	Capacitance per node (J/K)
5 small boxes	Aluminum 6082	5	2
PCB	Copper	9	2
Connection stack	Copper	3	2

Table 4.4: Thermal couplings for the power system.

Part 1	Part 2	Conductance (W/K)
Small boxes	PCB	4
PCB	Connection stack	1
PCB	Rods	0.1

4.1.3 On Board Computer (OBC)

The On Board Computer is from ISIS and it is modelled as two PCBs stacked together as shown in Figure 4.4. The main PCB is coupled to the connection stacks and the cylinder supports that is in turn coupled with the daughter board. Finally the main electronic board of the OBC is supported by the rods running through. Table 4.5 shows the details of the material used for such a system along with the capacitances per node obtained. The optical properties used for this system is the material itself and no coating is applied as such. The conductances between the couplings mentioned are given in Table 4.6.

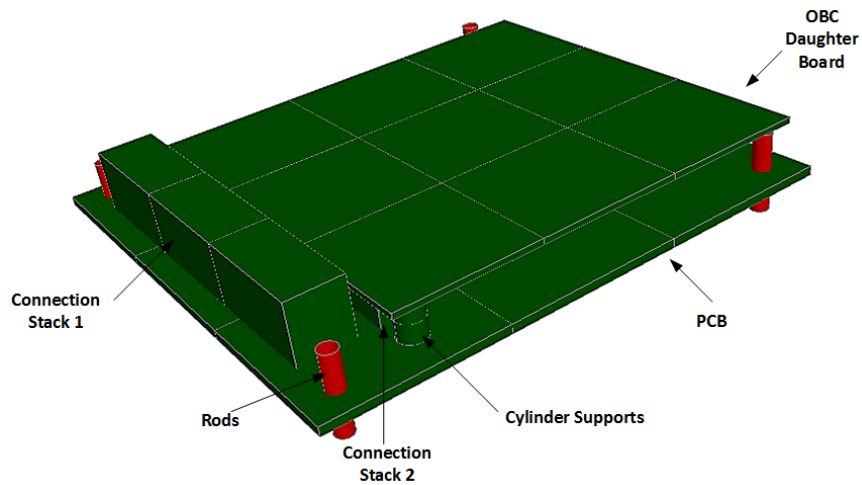


Figure 4.4: Thermal Model of ISIS OBC

Table 4.5: Model details for the OBC.

Name of the parts	Material used	Number of nodes	Capacitance per node (J/K)
Cylinder supports	Aluminum 6082	8	0.2
PCB	Copper	9	2
Connection stack 1	Copper	3	3
Connection stack 2	Copper	3	1
OBC daughter board	Copper	9	1

Table 4.6: Thermal couplings for the OBC.

Part 1	Part 2	Conductance (W/K)
Cylinder supports	PCB	2
PCB	Connection stack 1	1
PCB	Connection stack 2	1
PCB	Rods	0.1
Cylinder supports	OBC daughter board	2

4.1.4 ISIS Magnetorquer Board (iMTQ's)

The ISIS magnetorquer board is modelled as a flat PCB with thickness as shown in Figure 4.5. The torque rods are built perpendicular to each other and are attached to the thermal brackets. Here, the thermal brackets supporting the rods are modelled as thick plates with square cross section but the calculations for the couplings include the long slender brackets actually present in the original layout. The other couplings observed is between the PCB with the connection board and the aircore.

The material used is as represented in Table 4.7 along with the capacitances. The optical properties for the PCB is FR-4 and the other parts have no special coating included in this model. The thermal couplings calculated is as shown in Table 4.8.

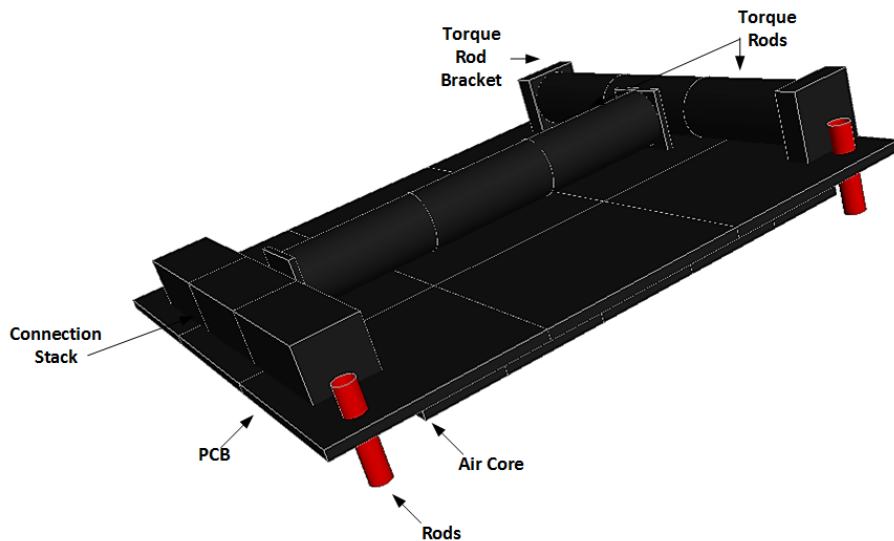


Figure 4.5: Thermal Model of ISIS Magnetorquer board

Table 4.7: Model details for the Magnetorquers.

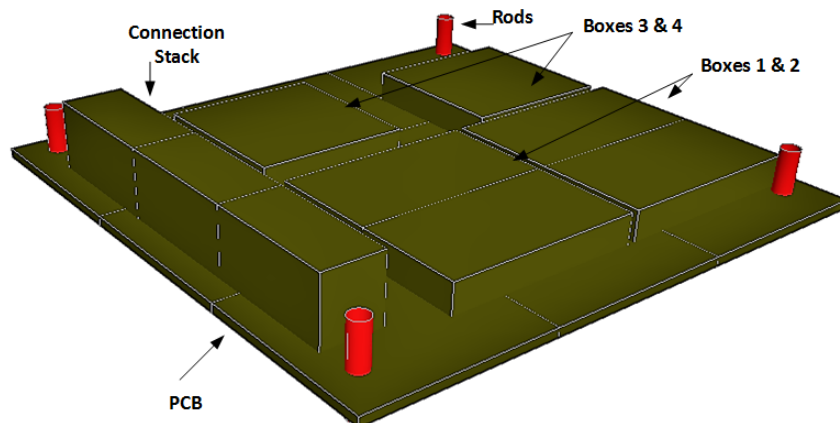
Name of the parts	Material used	Number of nodes	Capacitance per node (J/K)
Torque rods	Aluminum 6082	6	4
PCB	Copper	9	2
Torque rod 1 brackets	Aluminum 6082	2	0.2
Torque rod 2 brackets	Aluminum 6082	2	1
Connection stack	Copper	3	2
Air Core	Aluminum 6082	12	4

Table 4.8: Thermal couplings for the Magnetorquers.

Part 1	Part 2	Conductance (W/K)
Torque rod 1	Torque rod 1 bracket	1
Torque rod 2	Torque rod 2 bracket	1
PCB	Connection stack	1
PCB	Air core 1 and 3	9
PCB	Air core 2 and 4	8
PCB	Rods	0.1
PCB	Torque rod 1 bracket	0.3
PCB	Torque rod 2 bracket	1

4.1.5 TRXVU Transceiver

The TRXVU transceiver is also similarly modelled as others where it consists of a flat plate as a PCB, rectangular surface with thickness as connection stack and the other small boxes that are present on the PCB shown in Figure 4.6. Table 4.9 shows the materials used are copper for all components in this system.


Figure 4.6: Thermal Model of ISIS TRXVU- transceiver board

The thermal couplings observed are between PCB and connection stack, boxes 1,2,3 & 4, and lastly the structure rods as presented in the Table 4.10.

Table 4.9: Model details for the TRXVU transceiver.

Name of the parts	Material used	Number of nodes	Capacitance per node (J/K)
Boxes 1 and 2	Copper	4	4
Boxes 3 and 4	Copper	2	6
PCB	Copper	9	2
Connection stack	Copper	3	3

Table 4.10: Thermal couplings for the TRXVU transceiver.

Part 1	Part 2	Conductance (W/K)
PCB	Connection stack	1
PCB	Boxes 1 and 2	4
PCB	Boxes 3 and 4	6
PCB	Rods	0.1

4.1.6 Antenna system

The antenna system is a simple box like structure representing the antenna board which consists of the deployable antenna pointers shown in Figure 4.7. The antenna pointers are coupled with the board itself and the board in turn is modelled to be coupled with the ribs present just above the system. However, this connection between the ribs and the antenna system is not modelled geometrically but included in the conductive couplings.

Table 4.11 shows the capacitances per node for the parts mentioned. All the parts modelled are mostly made of copper and they are not specially coated other than the material itself. Table 4.12 shows the values for the conductive couplings obtained.

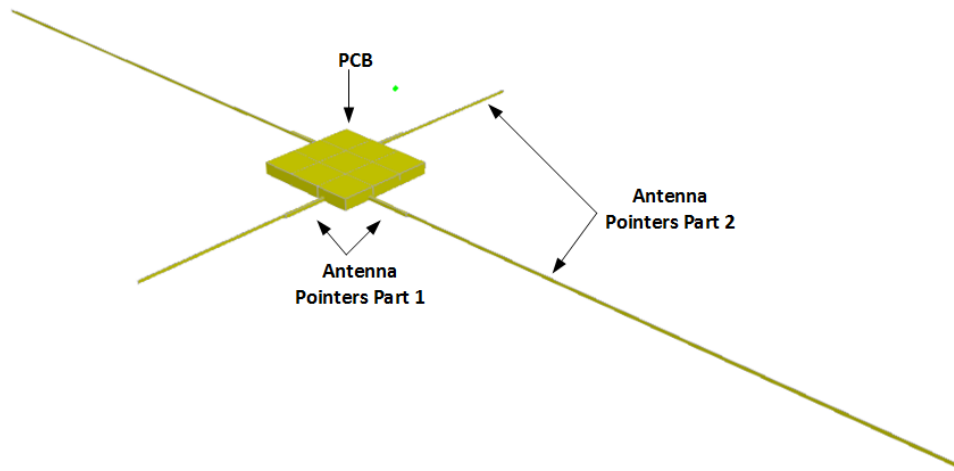


Figure 4.7: Thermal Model of ISIS antenna system

Table 4.11: Model details for the antenna system.

Name of the parts	Material used	Number of nodes	Capacitance per node (J/K)
Antenna pointer part 1	Copper	4	0.4
Antenna pointer part 2	Copper	2	0.1
Antenna pointer part 2	Copper	2	0.4
PCB	Copper	9	12

Table 4.12: Thermal couplings for the antenna system.

Part 1	Part 2	Conductance (W/K)
PCB	Antenna pointers part 1	0.4
Antenna pointers part 1	Antenna pointers part 2	3
PCB	Ribs	0.3

4.1.7 Solar Panels

The solar panels are classified as three different parts such as the deployable solar panels, 2U body mounted panels and 1U body mounted panels. All the panels are modelled as long flat plate with the thickness of $2mm$ as shown in Figure 4.8. These panels are

supported by the side-frames and structure ribs. The material used for the whole model is Aluminum 6082. The optical properties considered are Aluminum 6082 layer along with the solar cells on the positive outside and black anodized layer on the negative inside. The materials used and the capacitances are shown in Table 4.13.

The thermal couplings between the panels and the structure ribs along with the side-frames are tabulated in Table 4.14.

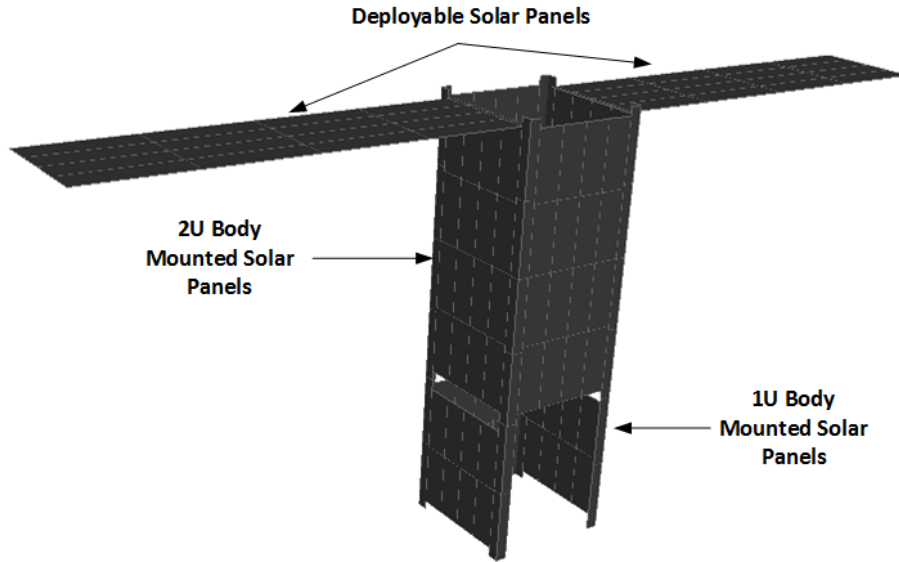


Figure 4.8: Thermal Model of ISIS solar panels

Table 4.13: Model details for the Solar panels.

Name of the parts	Material used	Number of nodes	Capacitance per node (J/K)
Deployable solar panels	Aluminum 6082	32	8
2U Body mounted panels	Aluminum 6082	64	5
1U Body mounted panels	Aluminum 6082	24	5

Table 4.14: Thermal couplings for the Solar panels.

Part 1	Part 2	Conductance (W/K)
Deployable solar panels	Structure ribs	0.3
2U and 1U solar panels	Sideframes	1

4.1.8 CubeProp

The NanoSpace CubeProp is a propulsion module consisting of thrusters and hence it is positioned at the top of the CubeSat for easier maneuverability. The thermal model consists of a large cylindrical propellant tank in the middle along with the interface and the main electronic boards supported by small cylinder supports. This tank is positioned properly on a mounting board with the help of screw interfaces on four sides. This interface is not modelled geometrically but considered while obtaining the conductive couplings. Figure 4.9 shows the thermal model of the CubeProp.

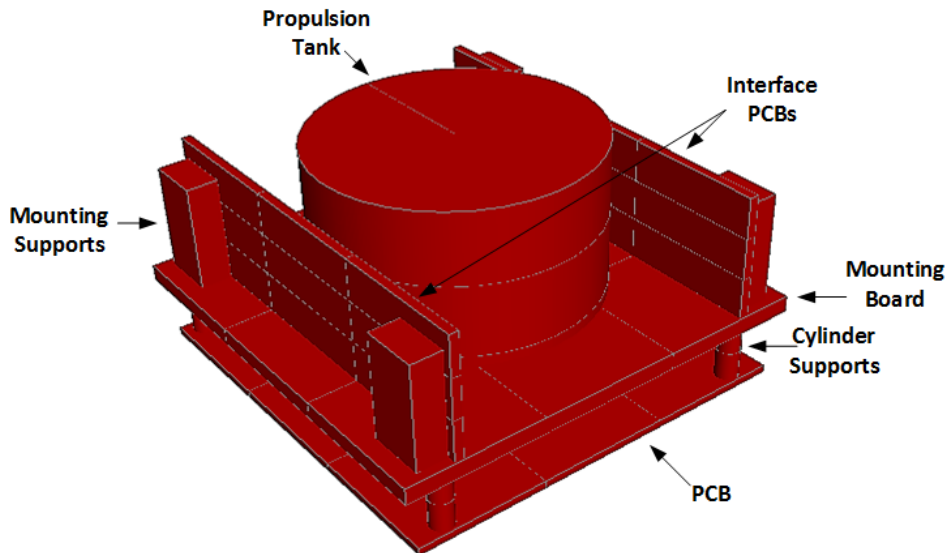


Figure 4.9: Thermal Model of NanoSpace-CubeProp

Table 4.15: Model details for the CubeProp.

Name of the parts	Material used	Number of nodes	Capacitance per node (J/K)
Propulsion tank	Aluminum 6082	5	15
PCB	Copper	9	2
Mounting board	Aluminum 6082	8	8
Interface PCBs	Copper	18	1
Cylinder supports	Aluminum 6082	8	1
Mounting supports	Aluminum 6082	4	6

The optical properties used as a coating for all the parts plays an important role in thermal activity of the system. These properties can be varied by using different tapes

on the surfaces. The electronic boards such as the PCBs are FR-4, the mounting board and all kinds of supports along with the tank are of Aluminum 6082. But this coating is later changed for some of the parts during the thermal control analysis to maintain the temperature limits. Table 4.15 shows the values for capacitance for each of the parts modelled in thermica. The thermal couplings observed in this model are mainly between the tank and the mounting board, supports with the mounting board and PCB with the structure rods. Table 4.16 shows the conductance values for all the couplings in detail.

Table 4.16: Thermal couplings for the CubeProp.

Part 1	Part 2	Conductance (W/K)
PCB	Cylinder supports	1
Mounting board	Cylinder support	1
Mounting board	Interface PCBs	2
Mounting board	Propulsion tank	0.1
Mounting board	Mounting support	1
Interface PCBs	Mounting supports	4
Mounting supports	Structure ribs	1
PCB	Rods	0.1

4.1.9 SEUD

The SEUD thermal model consists of the PCB and the connection stack as the main parts. The PCB is modelled as a flat plate of thickness $2mm$ and it is coupled to two separate flat boxes on the top and bottom. The connection stack is coupled with the PCB as shown in Figure 4.10. The optical properties are the same as the material used and no special coating is considered.

Table 4.17 shows the material considered for each part which is observed to be mostly copper. The thermal couplings between the parts are considered and obtained as shown in Table 4.18.

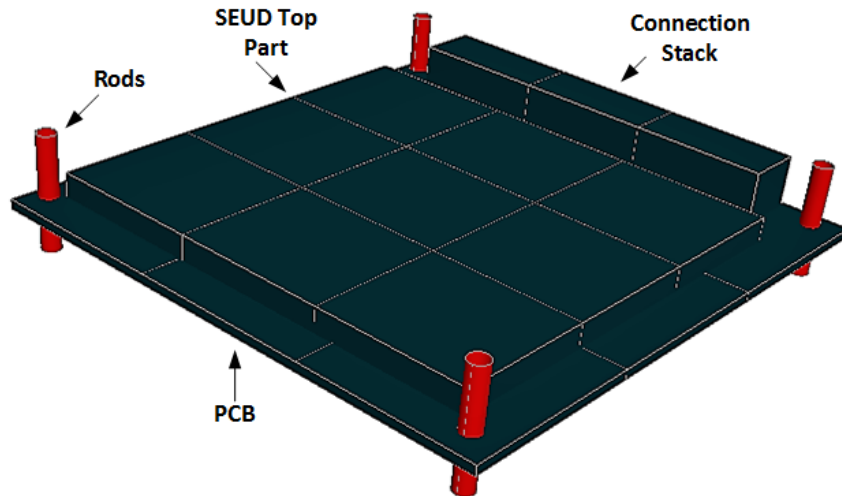


Figure 4.10: Thermal Model of SEUD

Table 4.17: Model details for the SEUD.

Name of the parts	Material used	Number of nodes	Capacitance per node (J/K)
SEU Top part	Copper	9	3
PCB	Copper	9	2
SEU Bottom part	Copper	9	4
Connection stack	Copper	3	2

Table 4.18: Thermal couplings for the SEUD.

Part 1	Part 2	Conductance (W/K)
PCB	SEU Top part	5
PCB	SEU Bottom part	4
PCB	Connection stack	1
PCB	Structure rods	0.04

4.1.10 MOREBAC

The MOREBAC is a biological experiment placed below the SEUD payload in the upper stack. The thermal model of this payload is just simple two boxes of different thickness. The detailed model of the payload is not yet available as the experiment is still in its developmental stage. As a result of this, detailed information regarding the materials or optical properties used are still not available. As for the analysis, the assumption made for one of the boxes is considered to be copper where as the other one is Aluminum 6082. This assumption was merely made based on the fact that MOREBAC intends to use PCBs and a tank to store the bacterias. This design is only to get a fair idea about the temperature limits for this experiment. The thermal model of the experiment is shown in Figure 4.11.

The capacitances for each of these materials are calculated based on the information assumed and can be seen from Table 4.19. The thermal couplings exist between the two boxes and one of the boxes is coupled with the structure rods for support. The values presented in Table 4.20 shows the conductances.

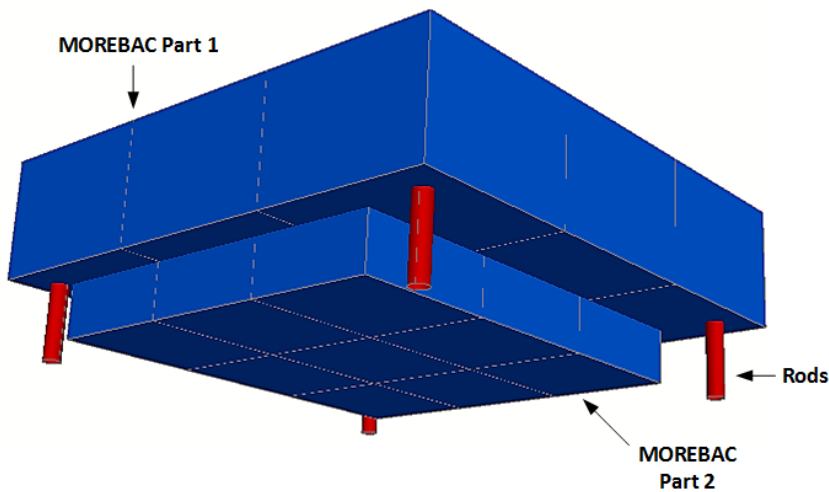


Figure 4.11: Thermal Model of MOREBAC

Table 4.19: Model details for the MOREBAC.

Name of the parts	Material used	Number of nodes	Capacitance per node (J/K)
MOREBAC Part 1	Copper	9	24
MOREBAC Part 2	Aluminum 6082	9	15

Table 4.20: Thermal couplings for the MOREBAC.

Part 1	Part 2	Conductance (W/K)
MOREBAC Part 1	MOREBAC Part 2	2
MOREBAC Part 1	Structure rods	0.1

4.1.11 RATEX-J

The RATEX-J is a particle detector experiment which is placed in the lower stack of the CubeSat and is exposed to space. This thermal model is fairly detailed and consists of many parts. Hence this model has the most number of couplings. It consists of two cylindrical shaped detectors placed in the -X direction. These detectors are coupled with the PCBs inside and together are coupled with the bottom panel. The panels cover the entire experiment on all sides as shown in Figure 4.13. The lower panel is coupled with the structure rods. There are other electronic boards which are modelled as boxes and also coupled with the lower panel inside. Figure 4.12 shows the inside view of the experiment module. All the parts of the RATEX-J has specific materials from which they are made of but since most of the parts are PCBs, they are modelled as copper. The Table 4.21 shows the details of the materials and capacitances for each of the modelled parts.

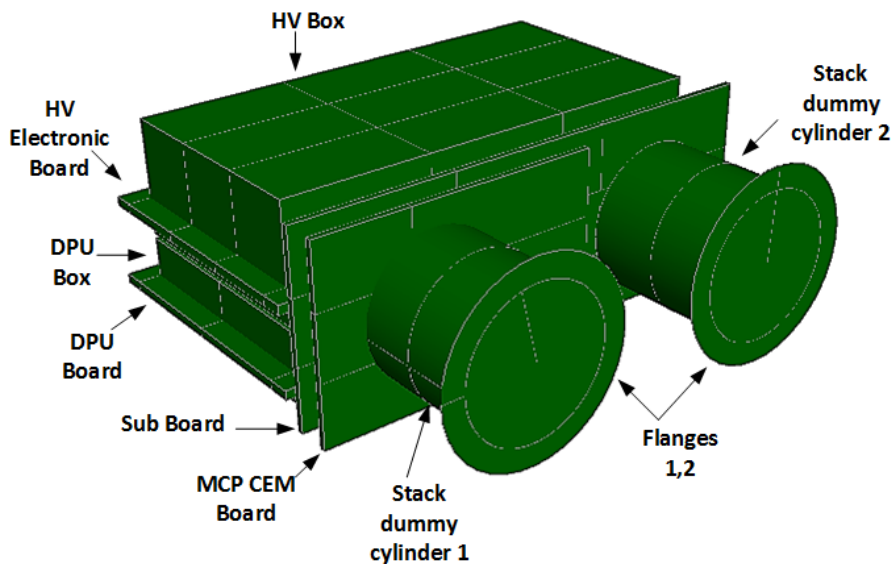


Figure 4.12: Thermal Model of RATEX-J (Inside View)

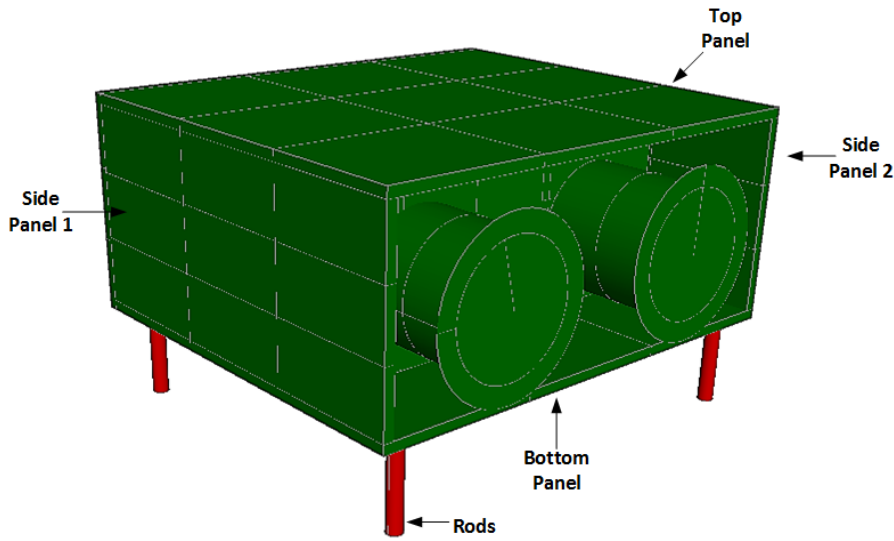


Figure 4.13: Thermal Model of RATEX-J

Table 4.21: Model details for the RATEX-J.

Name of the parts	Material used	Number of nodes	Capacitance per node (J/K)
Stack dummy cylinder 1,2	Aluminum 6082	4	10
MCP CEM Board	Copper	9	0.4
Sub Board	Copper	9	0.3
Stack dummy 1,2 Flanges	Aluminum 6082	2	2
SSD Box	Aluminum 6082	4	5
SSD electronic board	Copper	8	0.2
HV Box	Aluminum 6082	9	21
HV electronic board	Copper	12	0.3
DPU Box	Aluminum 6082	4	20
DPU electronic board	Copper	8	0.3
Side panel 1,2	Aluminum 6082	9	2
Bottom Panel	Aluminum 6082	9	5
Top panel	Aluminum 6082	9	5
Back panel	Aluminum 6082	9	2

The various couplings and conductance values are completely listed in Table 4.22.

Table 4.22: Thermal couplings for the RATEX-J.

Part 1	Part 2	Conductance (W/K)
MCP CEM Board	Top panel	0.1
MCP CEM Board	Stack dummy cylinder 1	2
Sub Board	Top panel	0.1
Sub Board	Stack dummy cylinder 1	0.02
SSD Box	SSD electronic board	0.3
SSD Box	Top panel	7
HV Box	HV electronic board	1
HV Box	DPU Box	4
HV Box	SSD Box	2
DPU Box	DPU electronic board	1
DPU Box	Top panel	14
Side panel 1,2	Bottom panel	2
Side panel 1,2	Top panel	2
Side panel 1,2	Back panel	0.3
Bottom panel	Back panel	1
Top panel	Back panel	1

4.1.12 SIC

The SIC experiment is modelled as a simple electronic board with thickness $2mm$ as shown in Figure 4.14. The material of the board is copper and no special coating is considered which can be seen in Table 4.23 along with capacitances per node. The thermal coupling shown in Table 4.24 is only between the board and the structure rods as of now because the final design of the experiment is yet to be completed.

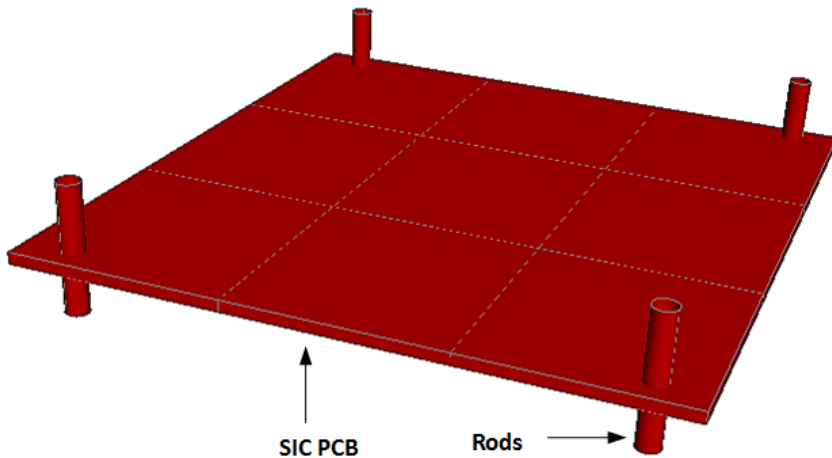


Figure 4.14: Thermal Model of SIC

Table 4.23: Model details for the SIC.

Name of the parts	Material used	Number of nodes	Capacitance per node (J/K)
SIC PCB	Copper	9	2

Table 4.24: Thermal couplings for the SIC.

Part 1	Part 2	Conductance (W/K)
SIC PCB	Structure rods	0.1

4.1.13 CUBES

The CUBES payload is also a particle detector experiment and is placed just below the RATEX-J in the lower stack of the CubeSat. It is modelled having three cubes which are coupled with the electronic board. This electronic board is in turn coupled with the structure rods. The thermal model shown in Figure 4.15. The material used is Aluminum 6082 for the cubes and copper for the PCB. The Table 4.25 shows the capacitances for each of the parts.

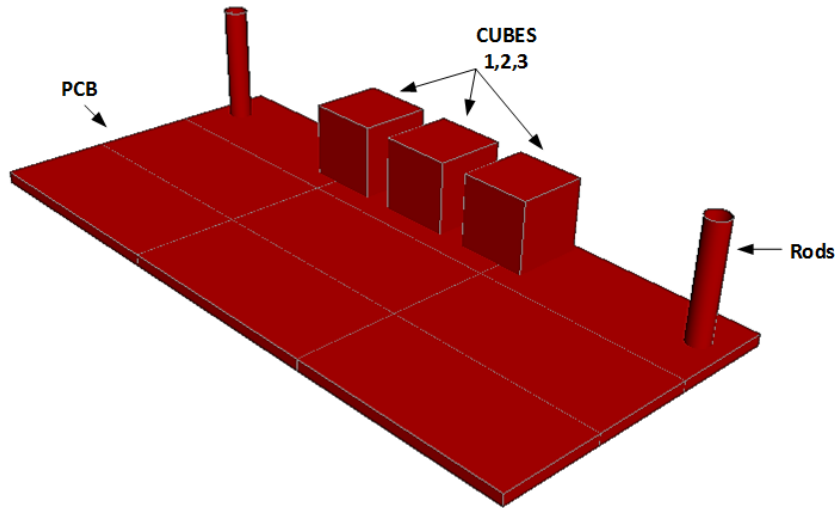


Figure 4.15: Thermal Model of CUBES

Table 4.25: Model details for the CUBES.

Name of the parts	Material used	Number of nodes	Capacitance per node (J/K)
Cube 1,2,3	Aluminum 6082	3	3
CUBES PCB	Copper	9	1

The thermal couplings as described are obtained as shown in Table 4.26.

Table 4.26: Thermal couplings for the CUBES.

Part 1	Part 2	Conductance (W/K)
CUBES PCB	Cube 1,2,3	2
CUBES PCB	Structure rods	0.01
CUBES PCB	Mounting plate	7

4.1.14 LEGS

The Piezo-LEGS experiment is modelled as two separate parts as shown in Figure 4.16. The first part is the electronic driver board which controls the Piezo motor. The second

part is the Piezo motor modelled as several boxes. Both the parts are fixed on the mounting board. The material and the capacitances are shown in Table 4.27.

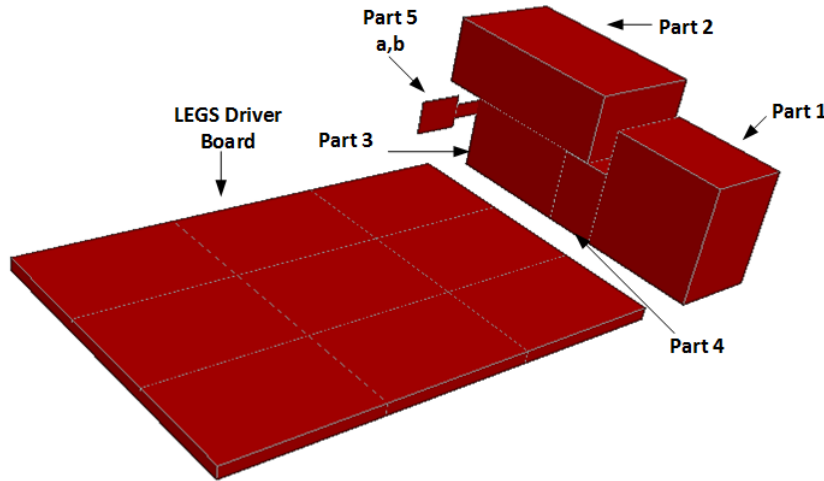


Figure 4.16: Thermal Model of Piezo-LEGS

Table 4.27: Model details for the Piezo-LEGS.

Name of the parts	Material used	Number of nodes	Capacitance per node (J/K)
Piezo motor part 1	Aluminum 6082	1	7
Piezo motor part 2	Aluminum 6082	1	11
Piezo motor part 3	Aluminum 6082	1	7
Piezo motor part 4	Aluminum 6082	1	1
Piezo motor part 5a	Aluminum 6082	1	0.01
Piezo motor part 5b	Aluminum 6082	1	0.02
LEGS Driver Board	Copper	9	0.4

The main coupling is between the driver board and the mounting board, the boxes used for the Piezo motor and the mounting board. The couplings along with their conductances are shown in Table 4.28.

Table 4.28: Thermal couplings for the CUBES.

Part 1	Part 2	Conductance (W/K)
Piezo motor part 4	Piezo motor part 1	1
Piezo motor part 4	Piezo motor part 3	1
Piezo motor part 2	Piezo motor part 3	6
Piezo motor part 3	Piezo motor part 5a	3
Piezo motor part 5a	Piezo motor part 5b	0.02
LEGS Driver Board	Mounting Board	5
Piezo motor part 1	Mounting Board	3
Piezo motor part 4	Mounting Board	1
Piezo motor part 3	Mounting Board	9
Driver Board	Structure rods	0.02

4.1.15 Camera

The Camera used is Raspberry Pi and is modelled as two parts as shown in Figure 4.17. The first part contains the Raspberry pi camera with the lens holder and the second part is just the Raspberry Pi board. This payload is placed at the lower stack facing the Earth i.e, -Z direction. No special optical properties are used except for their materials. The couplings observed are between the camera lens holder and the PCB, the Raspberry Pi board and the cover plate placed below the two parts for supports. Table 4.29 shows the materials considered for each of the parts and the obtained capacitances for each of them.

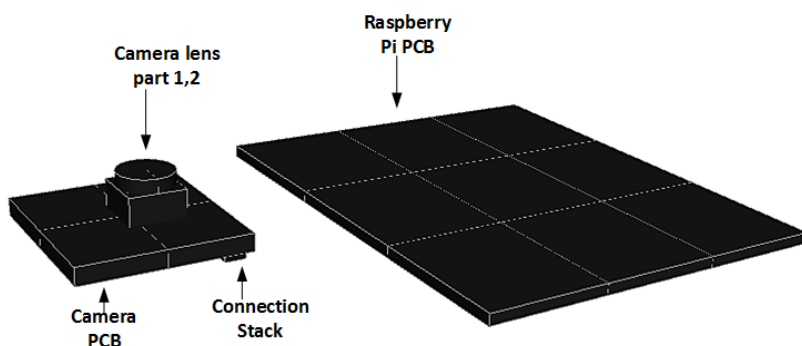
**Figure 4.17:** Thermal Model of Camera

Table 4.29: Model details for the Camera.

Name of the parts	Material used	Number of nodes	Capacitance per node (J/K)
Camera PCB	Copper	4	0.4
Connection stack	Copper	2	0.1
Camera lens part 1	Aluminum 6082	1	1
Camera lens part 2	Aluminum 6082	1	0.3
Raspberry Pi PCB	Copper	9	1

The thermal couplings mentioned earlier are represented in Table 4.30.

Table 4.30: Thermal couplings for the Camera.

Part 1	Part 2	Conductance (W/K)
Camera PCB	Connection stack	1
Camera PCB	Camera lens part1	1
Camera lens part 1	Camera lens part 2	3
Cover plate	Camera PCB	2
Cover plate	Raspberry Pi PCB	9

5

Thermal Analysis of MIST CubeSat

Once the thermal model is completely built, the next step for a thermal engineer is to simulate the model by applying right boundary conditions. The trajectory of the MIST CubeSat is at an altitude of 640 Km and its velocity direction is -X along the orbit. Figure 5.1 shows the MIST CubeSat (not to scale) having a nadir pointing along the described orbit. This chapter deals with the analysis of the MIST thermal model by implementing the heat dissipations on the components and simulating the model for different thermal cases. The hot and cold cases are main cases simulated to check the temperature behaviour of the satellite.

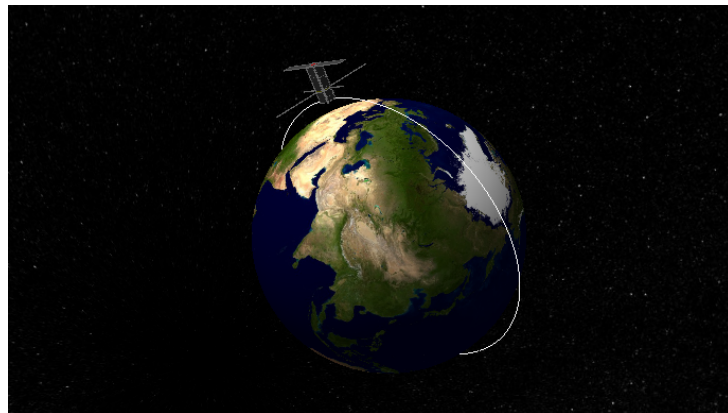


Figure 5.1: Trajectory of the MIST

5.1 Thermal Requirements for MIST

The temperature requirements for each of the units in MIST are different and through this thermal analysis, the requirements have to be met. Hence before starting with the simulations, this section introduces the various requirements put forth by the experimenters and the companies for all the payloads and subsystems. Table 5.1 shows the list of components and their node numbers along with temperature requirements that are need to be met.

Table 5.1: Temperature requirements for MIST Components.

Name of the Components	Node numbers	Operating Temperatures °C	Non-operating Temperatures °C
Solar panels	[100 - 347]	[-170,+130]	[-170,+130]
CubeProp	[1000 - 1603]	[+10,+50]	[-10,+60]
SEUD	[2000 - 2308]	[0,+85]	[-65,+150]
MOREBAC	[3000 - 3108]	[+20,+30]	[+4,+30]
RATEX-J	[4000 - 5608]	[-20,+20]	[-40,+50]
SIC	[6100 - 6108]	[-40,+105]	[-40,+105]
LEGS	[6200 - 6208]	[+10,+40]	[-30,+70]
	[6700 - 6910]		
CUBES	[6300 - 6608]	[+20,+30]	[-20,+80]
Camera	[7000 - 7408]	[0,+70]	[0,+70]
NanoPower P31-us	[9000 - 9600]	[-40,+85]	[-40,+85]
Battery	[10000-10502]	[-5,+45]	[-5,+45]
Magnetorquers	[11000 - 11702]	[-40,+70]	[-40,+70]
TRXVU transceiver	[12000 - 12500]	[-40,+60]	[-40,+60]
OBC	[13000 - 13408]	[-40,+60]	[-40,+60]
Antenna Board	[14000 - 14131]	[-30,+70]	[-30,+70]

During the analysis, there are always modelling errors and inaccuracies present which has to be accounted for at the end. Hence to be on the safer end, the final temperatures calculated are inclusive of the uncertainties as well. The margin placed for the raw temperatures obtained can vary from 5°C to 10°C depending on the necessity [29]. Figure 5.2 shows the temperature definitions considered before moving on to the thermal control analysis.

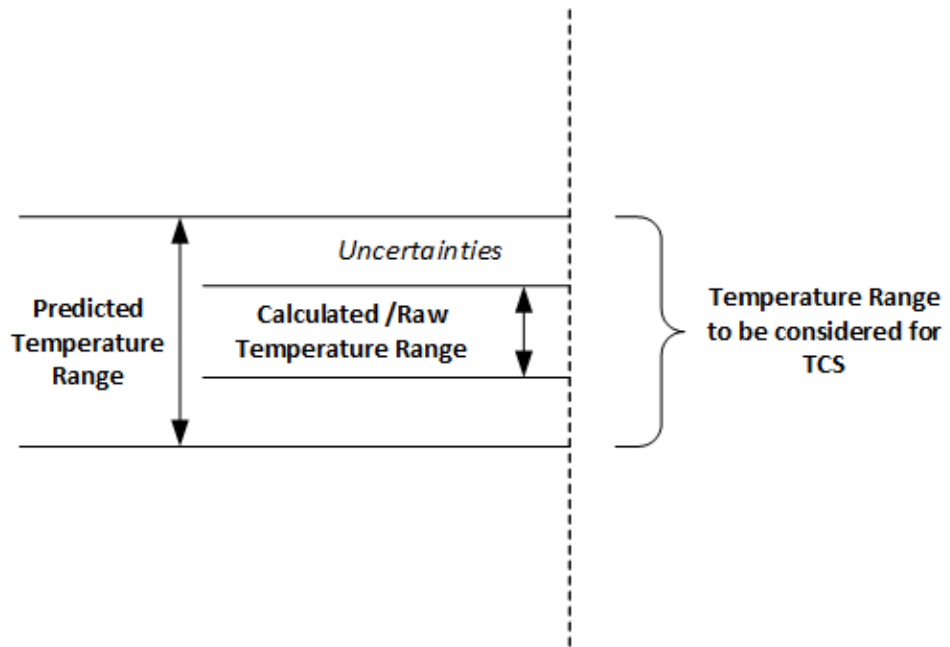


Figure 5.2: Temperature definitions for Thermal Control System (TCS)

The margin is set at $10^{\circ}C$ on both the maximum and minimum temperatures for all the units in MIST CubeSat. On designing a Thermal Control System (TCS) based on the temperature including uncertainties, it can be made sure that all the units in the CubeSat are under safe temperature limits.

5.2 Internal Heat Dissipation

The thermal analysis of any satellite requires the data from the power budget for each of the components used. This data basically depicts the complete usage of each component present in MIST CubeSat. This is because each of the components have different power requirements and they are used at specific times in an orbit. Hence, it is important to know these details such that the heat dissipation can be applied at those specific times. Also, it is important to know where on the unit the dissipation take place in order to apply the dissipation accordingly. The MIST project, however, due to its developmental phase has an initial draft of how the dissipation profiles should look like. Hence, in this thesis work, only one of the scenario is built and assumed for the entire analysis. There are three different cases that are run, one is the worst operational hot case, the other one is the worst non operational cold case and finally the operational cold case which are discussed in the following section.

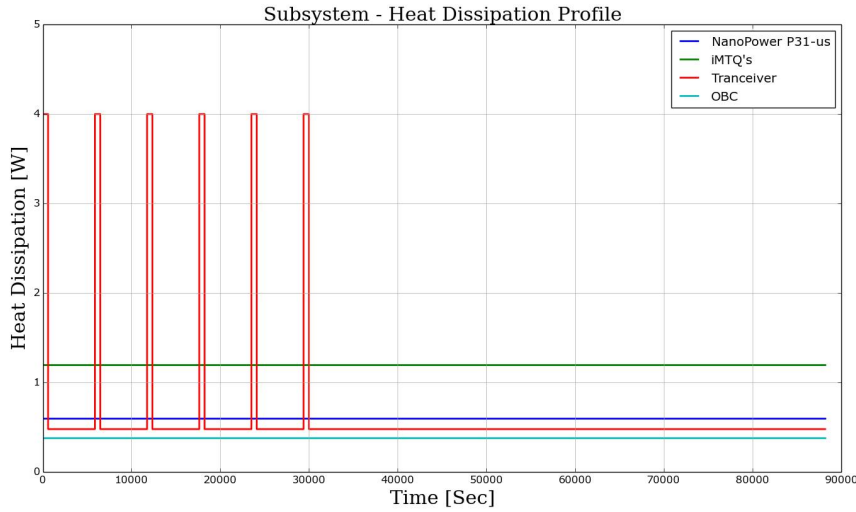


Figure 5.3: Subsystem-Heat Dissipation Profile

The Figure 5.3 shows the dissipation profile for the subsystems on board the satellite. These subsystems are always switched ON and hence are dissipating as long as the satellite is active. This is however different for the tumbling cases which are not dealt with here.

5.2.1 Operational Case

In this specific case, all the payloads in the MIST are operational and hence are dissipating. This dissipation profile consists of the heat loads acting on the satellite for the entire one day.

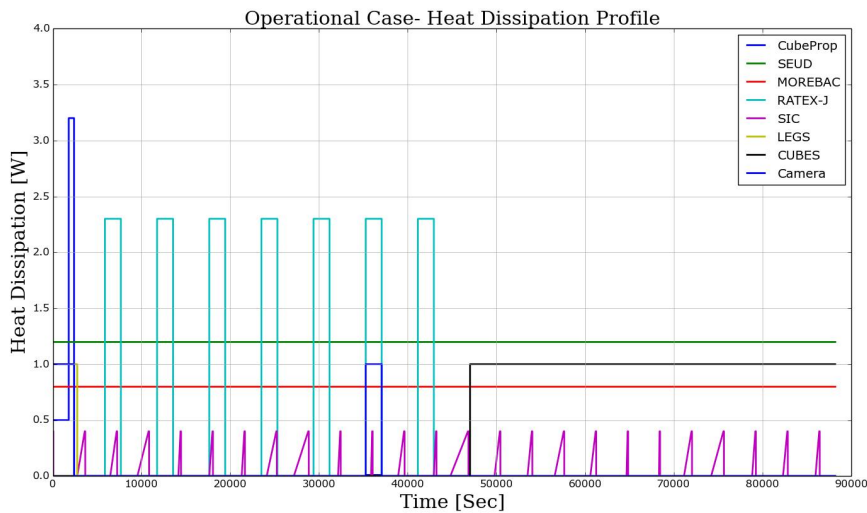


Figure 5.4: Operational Case-Heat Dissipation Profile

The Figure 5.4 shows the various dissipations for each of the payloads. The dissipation time for each of these payloads depend on the experiment requirements. The payloads such as SEUD, SIC and MOREBAC are seen to be continuously switched ON during the entire day where as the other payloads are kept ON for few of the orbits. This case is used both for hot case and cold case scenarios.

5.2.2 Non-Operational Case

In this case, the components which need to be active are still active like those of the batteries, AOCS, OBC, etc. as shown in the Figure 5.3. The payloads are however switched OFF and hence they are not dissipating any heat. The subsystems such as NanoPower P31-us, iMTQ's and the OBC are continuously switched ON throughout the orbital time whereas the tranceiver is switched ON only for the first few orbits which is based on the assumption that MIST CubeSat will cross over the ground station during that period of time.

5.3 Thermal model analysis

Apart from the operational or non operational cases, there are specific thermal cases such as hot and cold cases that are observed for temperatures. Thermal engineers adopt both these cases to define upper and lower bound temperatures observed for the satellite. These two cases are considered to be the worst thermal case scenarios and hence they are given importance. All the analysis performed here are for transient state conditions.

5.3.1 Hot Case

The hot case analysis is implemented by using the operational dissipation profile. This case corresponds to high dissipation of all the components in the CubeSat along with considerable amount of exposure to Solar, Albedo and Earth IR sources. Also the parameters used in case of MIST are LTAN of 22:30 and winter solstice of 2018 [2]. Here the LTAN value seems to be 15 minutes away from the original value of 22:45 to account for the extremes. During the winter solstice, the Earth is situated closest to the Sun. This is also found to be End of Life (EOL) case for the MIST CubeSat. The simulation for the thermal model is done for 15 orbits which means almost an entire day. Since this is the end of life analysis, the optical properties of all the materials will have to be changed in terms of absorptivity. This is due to accumulation of all the contamination on the coating over the large span of time resulting in forming a layer that absorbs more amount of radiation. This refers to thermal degradation of materials. The difference observed in absorptivity is taken from the Spacecraft Thermal Control Handbook by David G Gilmore.

5.3.2 Cold Case

The cold case analysis is implemented by using the non operational case where in all the payloads are switched OFF during this period. This is done to ensure that the temperatures are maintained even in non operational phase of the experiments. The parameters used are LTAN value of 23:00 and summer solstice of 2018 [2]. Similar to the hot case, the other extreme value of LTAN is considered here compared to the original. During the summer solstice, Earth is farthest from the Sun. This case is also found to be Beginning of Life (BOL) for the MIST CubeSat. All the optical properties of materials used are the BOL values or the initial values. This is because there are no significant changes in the optical properties due to degradation at the initial stages of the mission. Also the simulation of cold case when all the payloads are switched ON have also been performed using the same cold case environmental parameters. Apart from the two cases discussed here, there are also tumbling cases which come under this category as well. These tumbling cases does not come under the framework of the current thesis work but will be analysed later on as the project develops.

6

Thermal Control Design

Once the thermal analysis is completed, the temperatures obtained for the components have seemed to be exceeding the limits that they are supposed to be in. The main goal of thermal control system is to bring those temperatures down to accepted thermal limits. There are two types of thermal control such as the passive control and the active control system. The passive control is usually lighter in weight and cheaper compared to active control systems. MIST however needs both active and passive control systems for thermal control purposes. This chapter deals with the design of thermal control system for MIST and also discusses the implications it has on the overall design of the CubeSat.

6.1 Passive Control System

This type of thermal control does not involve any mechanical moving parts or moving fluids and also no power consumption. In fact passive means are the most suitable control system for a CubeSat because of its limited power budget constraints, low mass requirements and less complexity to design. Other than this fact it has also other advantages in terms of reliability and cost.

6.1.1 First Surface Mirrors

A First Surface Mirror (FSM) consists of a layer of metallic coating on a substrate as shown in Figure 6.1. These metallic coating have low emittance & absorptivity and typical coating used are aluminum or gold depending on the requirements. The substrate however is made out of polyimide film or FEP (fluorinated ethylene propylene) film [25].



Figure 6.1: Concept of First Surface Mirror (FSM) [25]

6.1.2 Second Surface Mirrors

When the Sun is shining on a surface, it will be heated and reach an equilibrium temperature based on the amount of sunlight absorbed and the amount of heat energy emitted. To reach lower equilibrium temperatures, another device is necessary with a lower absorptance to emittance ratio. A Second Surface Mirror (SSM) uses the bulk of the substrate to provide relatively high emittance and a metallic coating to provide low absorptance value [25]. For MIST, the lowest ratios of absorptance to emittance are obtained by using a Teflon film and a highly reflective silver coating to do the job. Figure 6.2 shows the concept discussed here.

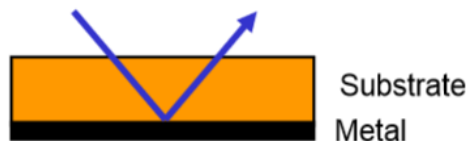


Figure 6.2: Concept of Second Surface Mirror (SSM) [25]

6.2 Active control System

In this type of thermal control system, mechanical moving parts and electrical power is required. The active means are preferred only when the temperature conditions exceed the limits on a larger scale. For instance, an heater might be required for heating the components up to required limits. The drawback of using this is that, it involves complex designs and requires extra electrical power and cost.

6.2.1 Heaters

The MIST CubeSat on the other hand requires heaters to bring the temperature conditions back to required conditions. Heaters are composed of electrical resistance elements that aid in the heating process. The later sections deals with the heaters applied to specific components in MIST.

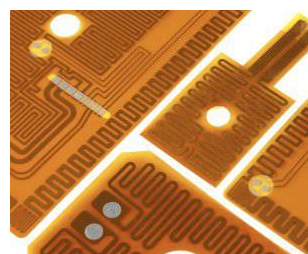


Figure 6.3: Typical heaters used for the satellites [26]

The commonly used heaters are the patch heaters shown in the Figure 6.3. As the heaters requirement is stated, this analysis consists of only the sizing of power requirements for the heaters and no specific heater chosen has been for the CubeSat yet.

6.3 Analysis results

This section is divided into three parts, cold non-operational case, hot operational case and lastly cold operational case results. The first two cases representing the worst case scenarios are discussed in detail along with the results whereas only the results are shown for the third case . These results are pertaining to only the components which are critical and most sensitive among the systems in the CubeSat. All the temperatures shown in the different cases are inclusive of the uncertainty considered.

6.3.1 Hot Operational Case :

The hot operational case can be considered as one of the worst case scenario where in all the subsystems and payloads are functional but the temperatures have to be limited to operating conditions. Figure 6.4 shows the observed temperatures compared with specified temperatures for each of the units with regard to hot case scenario. All the temperatures along with heater powers for the payloads and subsystems are shown in Table 6.1.

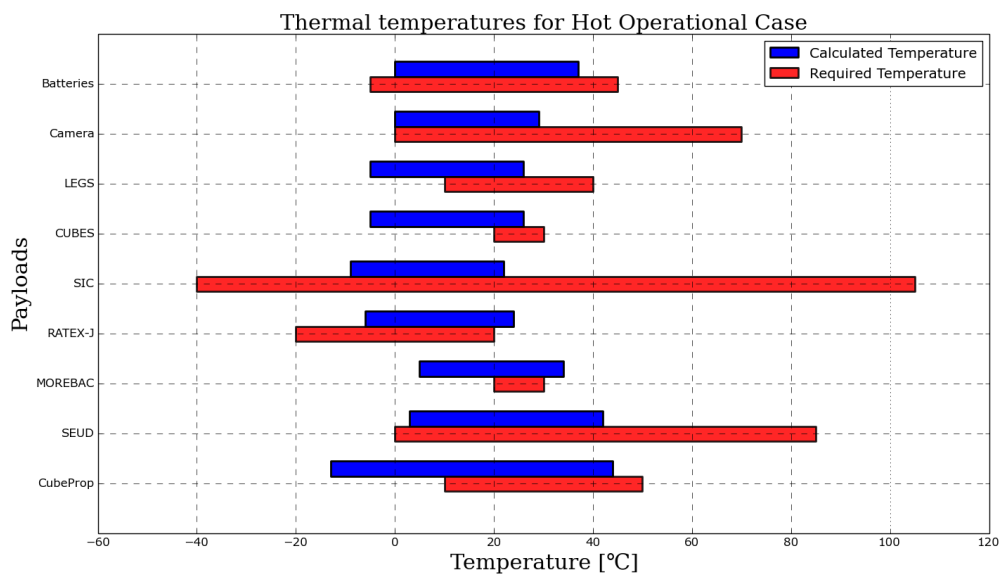


Figure 6.4: Temperature limit plot for Hot Operational Case

Table 6.1: Thermal temperatures for Hot Operational Case.

Payloads/ Subsystems	Required Temp. °C		Calculated Temp. °C		Average Heater Power/Day (W)
	Min.	Max.	Min.	Max.	
CubeProp	+10	+50	-13	+44	3.7
SEUD	0	+85	+3	+42	-
MOREBAC	+20	+30	+5	+34	-
RATEX-J	-20	+20	-6	+24	-
SIC	-40	+105	-9	+24	-
CUBES	+20	+30	-5	+26	-
LEGS	+10	+40	-5	+26	-
Camera	0	+70	0	+29	0.4
Batteries	-5	+45	0	+37	-

- **CubeProp**

The CubeProp is considered to be critical in this case because the tank being exposed to space and in the +Z direction, there is always a possibility to absorb more amount of solar radiation and hence, becomes hot. The material of the tank being aluminum 6082 which has a higher conductivity creates a problem. Hence, for this case, to lower the temperatures within the limit, the payload is covered by a cover plate placed on top to act as a barrier. Once this was designed, a layer of Teflon was coated on this cover plate along with the disc of the tank. The Teflon film along with the silver coating which had a thickness of 5 mil SSM was applied on the outer surface of the tank to limit the absorption of radiation. The propulsion tank is also coated with a same material but with a thickness of 10 mil SSM specifically to the top disc. There has been no taping used on the cylinder of the tank. This sort of passive thermal control system brought down the maximum temperature to within its limits. But the module as a whole is experiencing lower temperatures during the eclipse and has to be controlled. The propulsion tank, however, being the main concern with this experiment is under the temperature limits specified. The heater implemented earlier is still not optimized in such a way to control the temperatures on the minimum scale for the rest of the parts within. The average power required for the heater per day is around 3.7 Watts as of now.

- **SEUD**

SEUD is also simulated and observed that there is no exceed in limits on the hotter scale. The maximum temperature reached as seen in the table below is well within the limits but on the other hand the lower temperature scale during the eclipse

period is observed. But the heater implemented earlier is not required for this case. This is due to the fact that the heat conducted from the CubeProp is influencing the SEUD and hence maintaining it.

- **MOREBAC**

Since this is one of the critical unit among others, the temperature observed are beyond the limits mentioned by the experimenters. At the initial analysis it was observed that 1.2 Watts was seeming to high and rendering the temperatures high on the maximum scale. Since the experiment is still in its development phase, it was possible to change the power consumption. Once the dissipating power was reduced to 0.8 W, the conditions have seemed to be stabilized in terms of hotter scale. The heater used for this scenario earlier in the non operational case is switched OFF because it was observed to be over heating the equipment. But since the heater is switched OFF, the temperatures are also going well below on the minimum scale. Hence this experiment is very difficult to control on both the scales.

- **RATEX-J**

This payload is one of the passively controlled experiments. The temperatures observed before the implementation of the control system was that, it was experiencing hotter temperatures and had to be brought down. Hence, a Teflon film along with silver coating of thickness 10 mil SSM is applied on top panels of the experiment. It is later observed that even with the lower absorptance to emittance ratio, it is a bit hotter with respect to maximum temperatures.

- **SIC**

SIC is observed to be well within the temperature limits for the hot case as well. And hence no apparent changes or modifications have been performed.

- **CUBES**

CUBES is another experiment which has a narrower limits when it comes to operational case and hence is observed to be colder in this case. The heater implemented nearby is for the Camera but it seems to be critical. On increasing the heater power for the camera, the temperature for the RATEX-J is being affected due to conduction. Due to this reason there is no heater implemented near the RATEX-J. This is also the reason why the CUBES experiment is colder on the minimum scale.

- **Piezo LEGS**

This experiment is having the same problems as that of the CUBES. The hotter scale of the temperatures are just within the limits but colder scale is not able to reach the required specifications.

- **Camera**

The Camera payload is observed to be satisfying the thermal conditions . The heater implemented is controlling the minimum scale temperatures and its well within the boundary limits when it comes to hotter scale. The average power required for the heater per day is around 0.4 Watts.

- **Batteries**

The batteries being the most sensitive as mentioned earlier is also well within the thermal conditions. The heater is switched off and is not required for this case.

6.3.2 Cold-Non Operational case:

The Cold case non-operational case can also be considered the worst case scenario as of now wherein none of the payloads are functional but still has to be maintained within the non operational temperature limits. Note that the tumbling cases maybe one of the worst case scenarios but is not dealt with during this work. Figure 6.5 shows the observed temperatures compared with specified temperatures for each of the units with regard to cold non operational case scenario. All the temperatures along with heater powers for the payloads and subsystems are shown in Table 6.2.

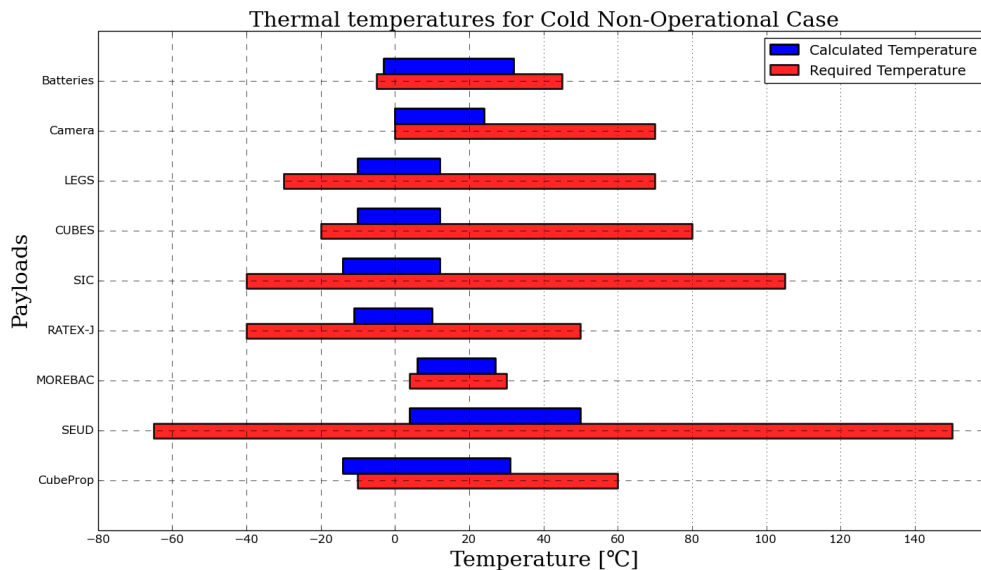


Figure 6.5: Temperature limit plot for Cold Non-Operational Case

Table 6.2: Thermal temperatures for Cold Non Operational Case.

Payloads/ Subsystems	Required Temp. °C		Calculated Temp. °C		Average Heater Power/Day (W)
	Min.	Max.	Min.	Max.	
CubeProp	-10	+60	-14	+30	3.0
SEUD	-65	+150	+4	+50	2.5
MOREBAC	+4	+30	+6	+27	1.7
RATEX-J	-40	+50	-11	+10	-
SIC	-40	+105	-13	+12	-
CUBES	-20	+80	-10	+12	-
LEGS	-30	+70	-10	+12	-
Camera	0	+70	0	+24	2.4
Batteries	-5	+45	-3	+31	-

- **CubeProp**

The Cubeprop is placed at the top of the CubeSat and is a bit exposed to space. The temperature conditions this payload is experiencing is very low temperatures compared to others. The integrated heater present in the experiment has a high resistance of 120 ohms and is placed at the bottom of the propulsion tank. The limitation of this heater is that with the high resistance, the heater power obtained is not enough or sufficient to do the job. Hence an additional heater was sized through this analysis to meet the requirements. The heater power sized is upto 6.5 Watts which seems to be a bit high but required. Once this heater is implemented the temperatures have come almost within the limits. From the observation it is seen that the tank of the propulsion module is completely well within the limits but the other parts of the component is bit colder. The average power required for the heater per day is around 3.0 Watts.

- **SEUD**

The SEUD payload is kept below the CubeProp and is only a PCB. This payload is also experiencing colder temperatures. This experiment does not contain any integrated heater but an additional heater is being taken in to account. The heater implemented for this experiment is sized to a power of about 5.5 Watts. Once this heater is activated on to this system, the temperatures are well within the requirements. The average power required for the heater per day is around 2.5 Watts.

- **MOREBAC**

MOREBAC is the third payload placed in the upper stack of the CubeSat. Since the design of this experiment is in process, the model contains only two boxes. But this experiment is one of the most sensitive compared to others in terms of temperatures and thus considered more important. This experiment is also equipped with a heater of power sized up to 3.9 Watts. During the non operational case, the temperatures can go lower than other cases and hence it is important for this experiment to maintain within limit so that the bacterias do not freeze. The results for this case is also reasonably within limits after implementing the heaters. The average power required for the heater per day is around 1.7 Watts.

- **RATEX-J**

RATEX-J payload is placed at the lower stack of the CubeSat and is a particle detector experiment which is exposed to space. The thermal model for this experiment is fairly detailed and this module seems to be maintained thermally without any application of heaters. The temperatures for this specific payload is well within the limits. There are no apparent changes made for this payload in the cold case.

- **SIC**

SIC is the silicon carbide experiment which is basically just the PCB. This payload however has wider temperature ranges between which it has to be maintained. There are no apparent changes made to this payload either in this case.

- **CUBES**

CUBES is another particle detector experiment placed just below the RATEX-J module in the lower stack. The thermal model is just a PCB and three cube shaped structures. The temperature limits for this case also seems to be fine and within the limits mentioned. Due to this reason there is no heater implemented to this module as well.

- **LEGS**

Piezo- LEGS is located close to the CUBES experiment in the lower stack itself. Both the CUBES and LEGS experiment are also exposed to space in the -X direction of the CubeSat. This payload is also well within the limits in the non operational case. There are no heaters implemented.

- **Camera**

The Camera is mounted on the cover plate pointing towards -Z direction at the lower stack. This payload is experiencing very low temperatures and hence an heater is designed. The heater implemented is sized up to a power of about 4.9 Watts and is positioned on the cover plate which is in contact with the camera and Raspberry Pi board. This heat that is supplied maintains the payload within the temperature

limits and also helps in maintaining the other payloads above it such as the CUBES, LEGS and SIC. The average power required for the heater per day is around 2.4 Watts. The heat conducted from the camera is also transferred to the other payloads such as CUBES and LEGS indirectly.

- **Battery**

The battery is another sensitive subsystem that is very crucial for the mission. Hence maintaining this temperature is of utmost important for the survival of CubeSat. There is already an integrated heater for the batteries. This heater has the power ranges of 3.5 to 5.9 Watts as mentioned in the ICD's and the minimum value of 3.5 Watts was considered. Since this is the non operational case wherein only the subsystems are switched on, there is always a possibility for the temperature to go down. The average power required for the heater per day is around 0.7 Watts.

6.3.3 Cold Operational Case:

The cold operational case has all the payloads and subsystems switched ON and are dissipating heat. The other parameters used are similar to the cold non operational case. The heaters power used for this case is same as that of the cold non operational case but the average power required per day may change according to the usage. Figure 6.6 shows the observed temperatures compared with specified temperatures for each of the units with regard to cold operational case scenario. From the Table 6.3 and 6.6 it can be observed that payloads CubeProp, MOREBAC, CUBES and LEGS are still not yet satisfied with regards to temperature limits whereas the rest of the payloads are within the requirements. All the heaters are switched ON in this case and the average power required are also mentioned in the Table 6.3. No changes in the thermal control system in terms of design are made for this case.

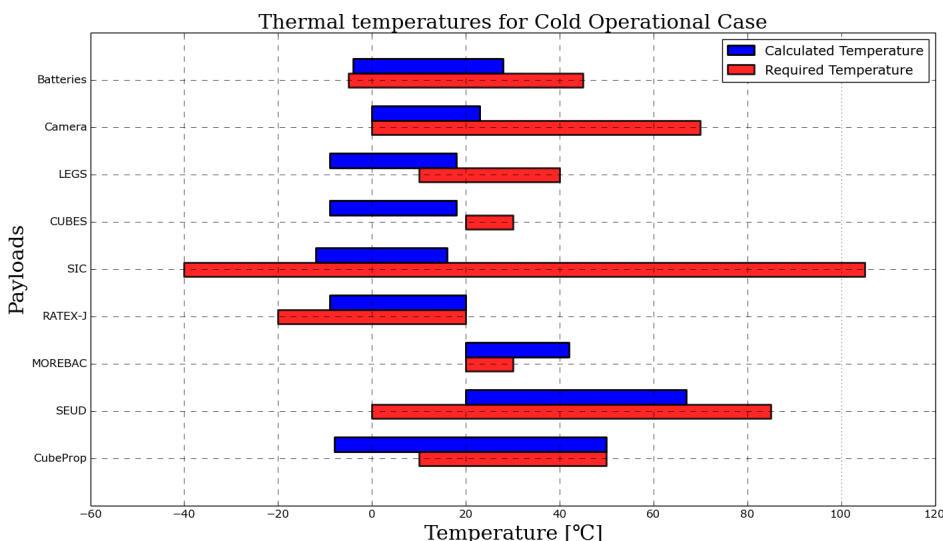


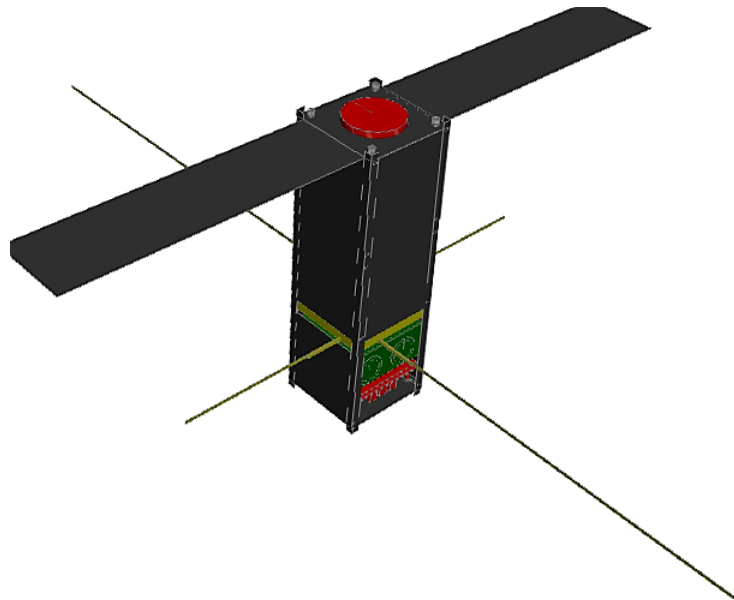
Figure 6.6: Temperature limit plot for Cold Operational Case

Table 6.3: Thermal temperatures for Cold Operational Case.

Payloads/ Subsystems	Required Temp. °C		Calculated Temp. °C		Average Heater Power/Day (W)
	Min.	Max.	Min.	Max.	
CubeProp	+10	+50	-8	+50	4.7
SEUD	0	+85	+20	+67	2.4
MOREBAC	+20	+30	+22	+42	2.3
RATEX-J	-20	+20	-9	+20	-
SIC	-40	+105	-12	+16	-
CUBES	+20	+30	-9	+18	-
LEGS	+10	+40	-9	+18	-
Camera	0	+70	0	+23	1.1
Batteries	-5	+45	-4	+28	0.2

6.4 New Thermal Model

After updating all the thermal control systems, the new design after considerations is shown in the Figure 6.7. This model consists of all the design changes made based on the results obtained from three cases that have been run.

**Figure 6.7:** New Thermal Model

7

CONCLUSIONS

7.1 Conclusion

This thesis work involved the understanding of basic principles behind the spacecraft thermal analysis and control. A detailed model of MIST CubeSat was modelled using the Thermica software to analyse the temperature variations for the entire satellite. The main intention through this work was to come up with a suitable control system that could maintain the thermal balance between the CubeSat and the space environment.

Due to the presence of many payloads and subsystems on board, it was necessary to ensure the overall reliability through this analysis. The work involved studying the temperature behaviour in three thermal cases such as cold case non operational, hot case operational and finally cold case operational. The first two cases were termed as the worst case scenarios and the thermal control system was built based on those analysis results. The TCS for the MIST involves both passive and active means of control. The upper bound temperatures experienced by the components were controlled completely using passive means such as Teflon Silvered coating on the surfaces. The lower bound temperatures required heaters to be controlled which was challenging in this case due to many components present in MIST. There were other design changes needed to be made such as introducing a cover plate for experiments like CubeProp and RATEX-J. As a result of these changes, the temperatures shown in the previous chapter are the final conditions observed.

Even after the application of these changes, it is observed that some of the payloads are yet to be brought under the requirements. Since the project is still in its developmental stages, further work could be done to control the temperatures and probably come up with an alternative design of TCS.

7.2 Future Work

Although the analysis was done on a detailed level, there are still many aspects that has to be considered as the time progresses. The materials used for each of the parts present

is assumed as of now due to incomplete information and hence has to be updated along with the optical properties.

The LTAN values need to be checked again for the mission because there seemed to be confusions with regard the values. One of the other main things to be looked into is the dissipation profile for each of the thermal cases. The analysis so far has only the assumed scenario but, after observing the results, it needs to be changed as the satellite is going too cold for the mission. The power dissipations and the location of where the dissipation is happening should be updated. As of now, the dissipations are applied to all the PCBs in the CubeSat.

Currently, the dissipation profile is just the basic one and with this the temperatures for all the payloads were colder than it needs to be. The thermal control analysis done for this scenario requires quite a few heaters and this could lead to power budget constraints. Hence, a new control design with less heaters could be beneficial. One of the methods is maybe to use the payloads or units to just dissipate heat by turning them ON when needed. Hence in this case the units or payloads in concern will be switched ON and dissipating heat but not operational. Such a mode can be useful in maintaining the temperature only if it is allowed by the experimenters. Also, the use of MLI could be one of the options to consider for some of the payloads.

Lastly, the location of the payloads such as the CUBES and Piezo LEGS are very critical. From this analysis it was observed that placing a heater for the CUBES or the LEGS, the temperatures for RATEX-J was being influenced. Hence this seems to be an issue that has to be addressed.

A

Geometrical Model Properties

This section entails all the material and thermo-optical properties pertaining to the detailed geometric model designed for the thermal analysis. All the values represented here are standard and belong to the materials used for each models.

A.1 Material Properties

Figure A.1 shows the various materials used for MIST CubeSat. The SolarPanels mentioned in the legend is same as the material Aluminum 6082 but with different optical properties. As seen from the Figure A.1 most of the CubeSat is composed of only Aluminium 6082 and Copper as of now.

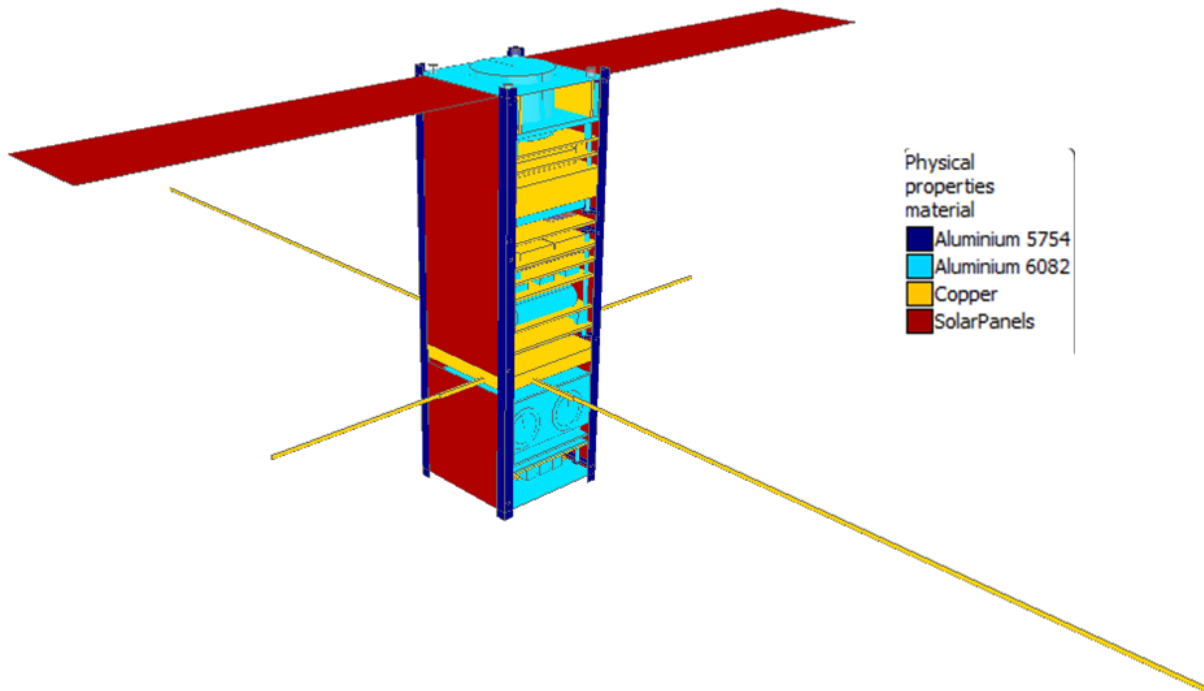


Figure A.1: Materials used for MIST CubeSat

Table A.1: Material properties used in geometric model. [1]

Material used	Specific heat Capacity($J/Kg.K$)	Density (Kg/m^3)	Conductivity (W/mK)
Aluminum 6082	896	2810	170
Aluminum 5754	900	2670	130
Copper	589	2223	20.5

Table A.1 shows the typical values used for the Specific heat Capacity, Density and Conductivity of the materials. These properties are very important to calculate the Capacitances for all the parts.

A.2 Optical Properties

Figure A.2 shows the various optical properties used for MIST CubeSat. As seen from the Figure A.2, there are some special coatings such as Teflon-Silvered, FR-4, Black Anodized layer have been applied to some of the surfaces as passive means to control the temperature.

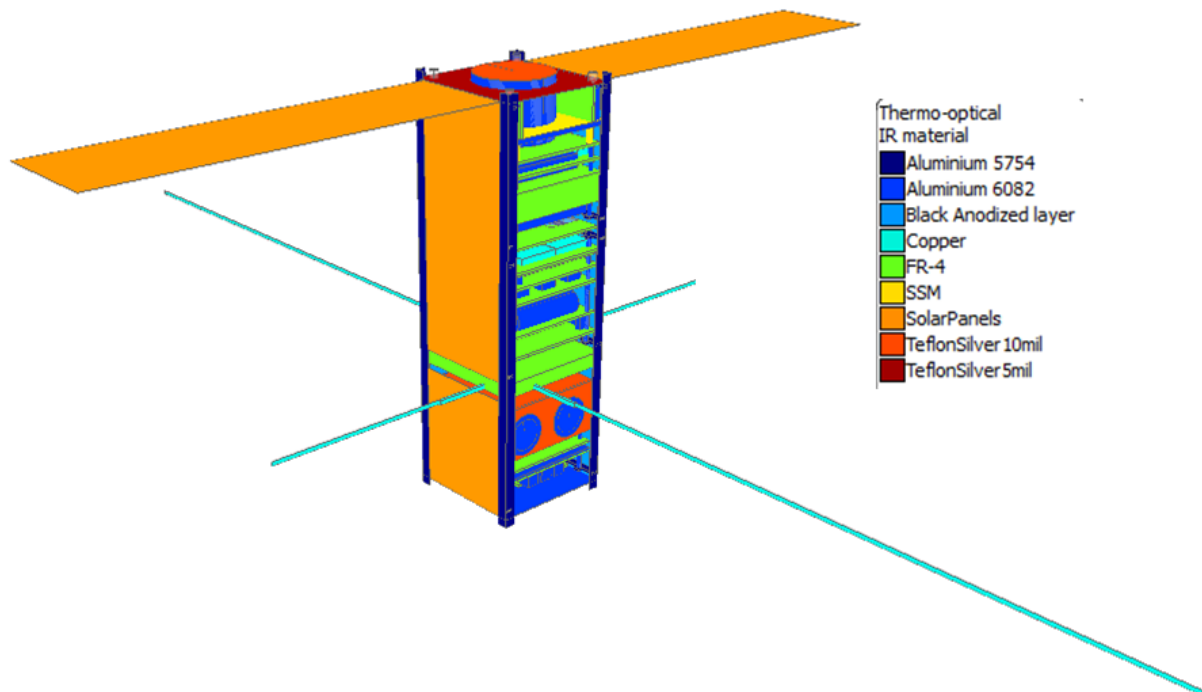
**Figure A.2:** Optical coatings used for MIST CubeSat

Table A.2: Optical properties used in geometric model. (BOL Values) [1]

Material	Emissivity	Absorptivity
Aluminum 6082	0.05	0.15
Aluminum 5754	0.82	0.65
Black Anodized Layer	0.88	0.76
Copper	0.8	0.9
FR-4	0.89	0.75
SSM	0.78	0.23
Solar Panels	0.86	0.6
Teflon Silvered 10 mil	0.88	0.09
Teflon Silvered 5 mil	0.81	0.08

Table A.2 shows the values of emissivity and absorptivity considered for BOL cases. The EOL values takes into consideration of the change in absorptivity due to thermal degradation. All these values are hereby taken from the Thermal Control Handbook by David G Gilmore.

The emissivity and absorptivity values for solar panels are calculated separately here. It is very important to consider the effective loss in absorptivity of solar cells due to the conversion of solar into electrical energy. This is shown as:

$$\alpha_{eff} = \alpha_{cell} - \mu_{cell} = 0.9 - 0.3 = 0.6 \quad (\text{A.1})$$

wherein μ_{cell} represents the maximum efficiency of the cell, α_{cell} is the absorptivity of the solar cells used and α_{eff} is the effective absorptivity. However this is the case for BOL cases but for the EOL case, the effective absorptivity can be calculated as :

$$\alpha_{eff} = \alpha_{cell} - 50\% * \mu_{cell} = 0.9 - 0.5 * 0.3 = 0.75 \quad (\text{A.2})$$

Due to the difference in conversion efficiency of solar cells during different thermal cases, a power draw of 100 % is considered for cold cases whereas 50 % for the hot cases [29]. The emissivity, however, remains constant throughout the life time of CubeSat. The effective emissivity can be calculated as :

$$\epsilon_{eff} = 31\% * \epsilon_{Al} - 69\% * \epsilon_{cell} = 0.31 * 0.88 - 0.69 * 0.85 = 0.86 \quad (\text{A.3})$$

wherein the ϵ_{Al} is the emissivity of the black anodized layer applied on the solar panel of material aluminum 6082. Also, it is considered that 69 % of the panels are covered with cells [27].

B

Internal Heat Dissipations

This section gives the details of peak power dissipations observed in each of the units present in MIST CubeSat. Refer MIST ICD's for more details. All the values represented here are the latest and may be further updated as the project develops. Table B.1 shows the values of power dissipation per payload during operating as well as idle conditions.

Table B.1: Power dissipation values for payloads during operating & idle conditions.

Payloads	Operating Power (W)	Idle Power (W)
CubeProp	3.2	0.01
SEUD	1.2	0.25
MOREBAC	1.2	-
RATEX-J	2.3	-
SIC	0.4	-
CUBES	1.0	-
LEGS	1.0	-
Camera	1.0	0.36

During the non operating conditions, all the mentioned payloads are switched OFF during which only the subsystems are switched ON. The power dissipations observed for the subsystems are shown in Table B.2

Table B.2: Power dissipation values for Subsystems during operating & idle conditions.

Subsystems	Operating Power (W)	Idle Power (W)
NanoPower P31-US	0.6	-
iMTQ's	1.2	0.15
Transceiver	4	0.48
OBC	0.38	-

C

Figures

The temperature variation within the MIST CubeSat is very important and it is based on these temperatures that the control system is developed. Figure C.1 shows the distribution of temperatures during the hot operational case at time zero. The temperature scale is also shown along with the CubeSat. Figure C.2 shows the temperature distribution for the cold non-operational case and Figure C.3 shows the distribution for cold operational case at time zero respectively. At time zero, the CubeSat seems to be in an eclipse phase and also crossing the equator in an ascending node.

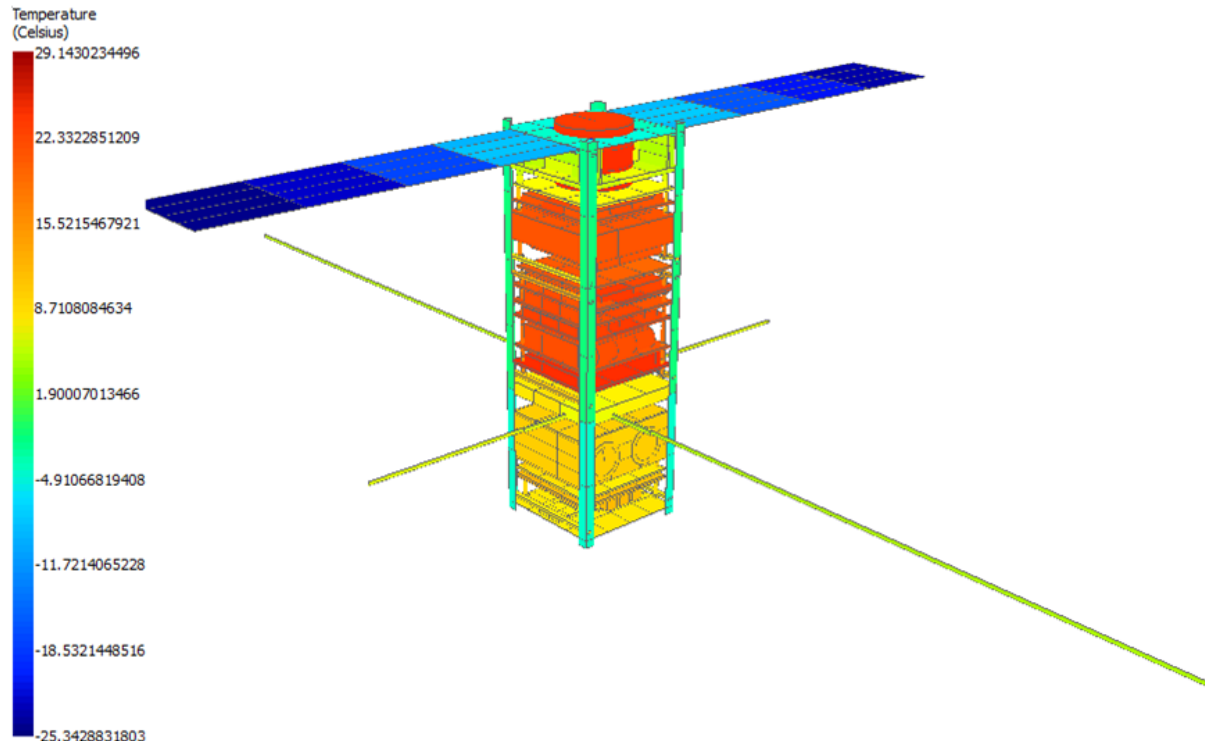


Figure C.1: Thermal temperatures of MIST CubeSat at time zero for the Hot Operational case

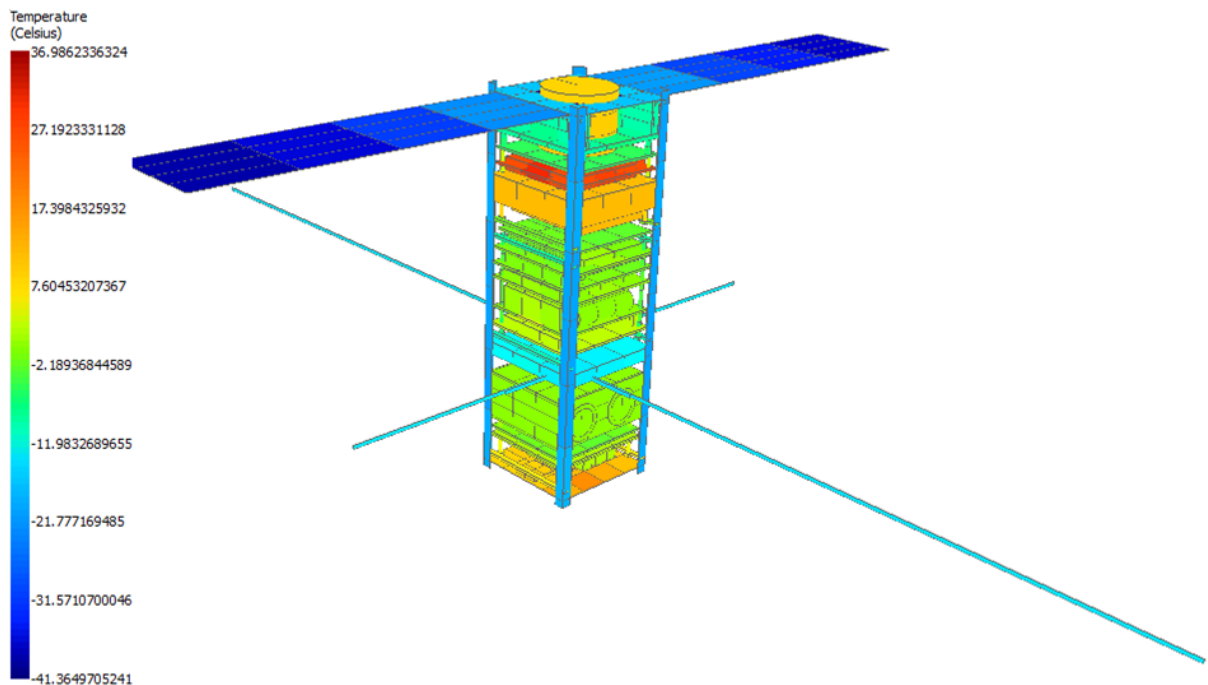


Figure C.2: Thermal temperatures of MIST CubeSat at time zero for the Cold Non-Operational case

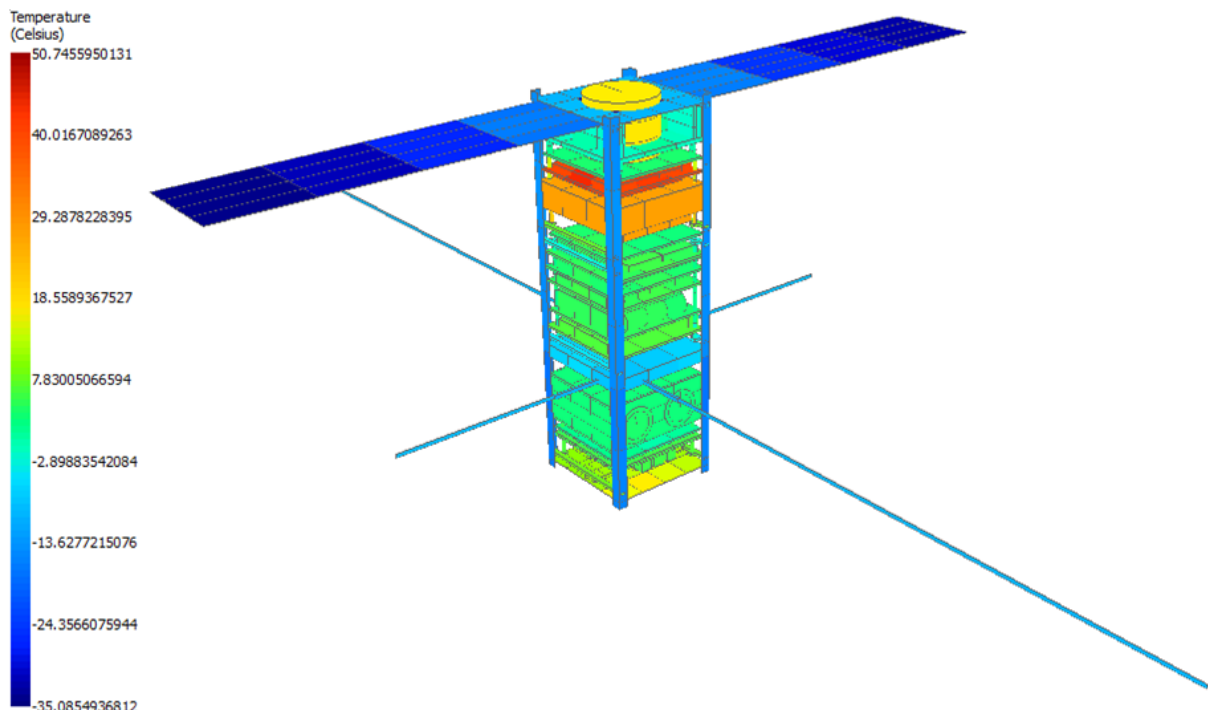


Figure C.3: Thermal temperatures of MIST CubeSat at time zero for the Cold Operational case

Bibliography

- [1] David G. Gilmore, *Spacecraft Thermal Control Handbook, Volume 1: Fundamental Technologies*, The Aerospace Press, American Institute of Aeronautics and Astronautics, Inc. 2002.
- [2] MIST, *Reference Orbit version 3*, Interface Control Documents, 2015.
- [3] Gomspace, *NanoPower BP4 battery pack*, <http://www.gomspace.com/documents/ds/gs-ds-nanopower-bp4-2.3.pdf>, 2015.
- [4] Gomspace, *NanoPower P31-us*, <http://www.gomspace.com/documents/ds/gs-ds-nanopower-p31u-13.pdf>, 2015.
- [5] Innovative Solutions In Space, *On Board Computer*, https://www.cubesatshop.com/wp-content/uploads/2016/06/ISIS_ISIS-OBC_Brochure_v.15.6.pdf, 2015.
- [6] Innovative Solutions In Space, *Magnetorquer Board*, <https://www.isispace.nl/product/isis-magnetorquer-board/>, 2015.
- [7] Innovative Solutions In Space, *TRXVU transceiver Board*, <https://www.isispace.nl/product/isis-uhf-downlink-vhf-uplink-full-duplex-transceiver/>, 2015.
- [8] Innovative Solutions In Space, *Deployable Antenna System*, https://www.isispace.nl/brochures/ISIS_AntS_Brochure_v.7.11.pdf, 2015.
- [9] MIST, *ISIS Solar Panel- Side Mount User Manual*, Interface Control Documents, 2012.
- [10] MIST, *NanoSpace version 3*, Interface Control Documents, 2015.
- [11] MIST, *SEUD version 2*, Interface Control Documents, 2015.
- [12] MIST, *MOREBAC version 3*, Interface Control Documents, 2015.
- [13] MIST, *RATEX-J version 2*, Interface Control Documents, 2015.
- [14] MIST, *SIC version 2*, Interface Control Documents, 2015.

- [15] MIST, *CUBES version 2*, Interface Control Documents, 2015.
- [16] MIST, *Piezo LEGS version 2*, Interface Control Documents, 2015.
- [17] MIST, *Camera version 3*, Interface Control Documents, 2015.
- [18] MIST, *ISIS CubeSat STructural Subsystem*, Interface Control Documents version 2.1, 2012.
- [19] MIST, *Coordinate Systems and Subsystem Orientations*, Document version 5, 2016.
- [20] R.Karam, *Satellite Thermal Control for Systems Engineers*, American Institute of Aeronautics and Astronautics, Inc. 1998.
- [21] Mike Legatt Dave Hauth, Chuck Hisamoto *Thermal Analysis*, University of Minnesota, 110 Union Street SE, Minneapolis, MN 55455, April 2008.
- [22] Yunus A. Cengel *Heat Transfer: A Practical Approach*, McGraw-Hill, Inc. 2003 .
- [23] Andreas Berggren, *Design of Thermal Control System for the Spacecraft MIST*, Department of Space and Plasma Physics, KTH Royal Institute of Technology, Sweden 2015.
- [24] Airbus Defense and Space “*Systema-Thermica*” <http://www.systema.airbusdefenceandspace.com/products/thermica.html>
- [25] Sheldahl, “*The Red Book*” <http://www.sheldahl.com/documents/Thermal%20Control%20Overview.pdf>
- [26] Active Control System, *Heaters*, <http://www.holroydcomponents.com/blog/everything-you-ever-wanted-to-know-about-kapton-heaters-but-were-afraid-to/>, 2016.
- [27] Tom van Boxtel *Thermal modelling and design of the DelFFi satellites*, Delft University of Technology, 2015.
- [28] Urmas Kvell, Marit Puusepp, Franz Kaminski, Jaan-Eerik Past, Kristoffer Palmer, Tor-Arne Gronland and Mart Noorma, "Nanosatellite orbit control using MEMS cold gas thrusters", Proceedings of the Estonian Academy of Sciences, 2014, 63, 2S, 279–285.
- [29] Andreas Berggren, *Standard Values for thermal design of satellites*, Surrey Satellite Technology Limited (SSTL), Uk.
- [30] Kavithasan Patkunam, *CAD Team Report-Team 3*, MIST, 2016.
- [31] Wikipedia, *Radiative View factor*.

